Master's thesis

NTNU
Norwegian University of Science and Technology
Faculty of Natural Sciences
Department of Chemical Engineering

Hanne Skudal Ullaland

Flocculation-on-a-chip: produced water studied by advanced microfluidic methods

Master's thesis in Chemical Engineering and Biotechnology
Supervisor: Gisle Øye, Marcin Dudek
July 2020

NTNU
Norwegian University of Science and Technology

Hanne Skudal Ullaland

Flocculation-on-a-chip: produced water studied by advanced microfluidic methods

Master's thesis in Chemical Engineering and Biotechnology
Supervisor: Gisle Øye, Marcin Dudek
July 2020

Norwegian University of Science and Technology
Faculty of Natural Sciences
Department of Chemical Engineering

NTNU
Norwegian University of
Science and Technology

Preface

This Master Thesis has been written as the final work of my studies in the Master's Degree Programme "Chemical Engineering and Biotechnology" at the Norwegian University of Science and Technology (NTNU).

I want to express my gratitude to my supervisor Professor Gisle Øye, for giving me the opportunity to work on this project. I am thankful for his guidance during the weakly meetings and the useful feedback on this thesis. I would also like to express my appreciation to my co-supervisor Marcin Dudek, for his support, guidance and patience throughout this project. I am grateful for the feedback and comments on this thesis and support in the laboratory.

I would also like to thank all the staff and employees at Ugelstad laboratory that helped me in the lab, and for valuable discussions and motivation.

I want to thank Per-Erik Hellberg and Alireza Movahedi from Nouryon, for providing the chemicals and for discussions and feedback during meetings throughout this project.

Trondheim, 01.07.2020

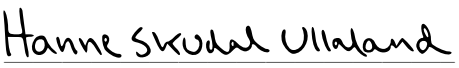

Hanne Skudal Ullaland

Abstract

Produced water, consisting of dispersed oil, is a substantial by-product from the hydrocarbon production. It is essential to remove the dispersed oil from the produced water before it can be discharged or re-injected, and, therefore, it needs to be treated. One way to boost the efficiency of the treatment is to promote the phenomena of coalescence and flocculation, which increase the oil droplet sizes and improve the separation. This can be achieved by the addition of production chemicals to the produced water, namely flocculants. Microfluidics is a relatively new method that can be used for the investigation of crude oil emulsion stability and the coalescence and flocculation of oil droplets.

This project aims to investigate different flocculants effect on crude oil emulsion stability with a microfluidic method; the Universal Microfluidic Platform apparatus. And, to develop an approach for a dynamic change of the flocculant concentration in the microfluidic setup. In addition, several methodologies for flocculant and emulsion characterization have been performed. These included measurements of size, zeta potential and surface tension of flocculant solutions, and zeta potential, interfacial tension and rheology measurements of crude oil emulsions. Besides, the turbidity of crude oil emulsions was measured over time to verify the results from the microfluidic method. The work is a continuation of the work performed during the course 'TKP4580 - Chemical Engineering, Specialization Project' fall 2019.

A crude oil from the Norwegian Continental Shelf was used for preparation of emulsions. The crude oil emulsions were investigated with and without the addition of eight different commercial flocculants. The studies showed that properties as size and zeta potential of the flocculant solutions play a role in the emulsion stability. Also, the addition of flocculants to the crude oil emulsions slightly affected the interfacial tension and rheology. From the experiments performed with the microfluidic technique, it was found that the results do, to some degree, correspond to the turbidity measurements. Also, a dynamic change of the flocculant concentration made it less time consuming to perform several tests, with comparable results. It is concluded that the microfluidic technique is a good option for the investigation of emulsion stability and that a dynamic change in the flocculant concentration is a satisfactory and time-effective method to perform experiments with the microfluidic technique.

Sammendrag

Produsert vann, bestående av dispergert olje, er et betydelig biprodukt fra oljeproduksjonen. Det er viktig å fjerne den dispergerte oljen fra det produserte vannet før det kan tømmes ut eller reinjiseres, og det produserte vannet må derfor behandles. En måte å forbedre effektiviteten av behandlingen på er å fremme fenomenene koalesens og flokkulering, som øker størrelsen av oljedråpene og forbedrer separasjonen. Dette kan oppnås ved tilsetning av produksjonskjemikalier til det produserte vannet, nemlig flokkulanter. Microfluidiks er en relativt ny metode som kan brukes til undersøkelse av råoljeemulsjoner og koalesens og flokkulering av oljedråper.

Dette prosjektet har som mål å undersøke forskjellige flokkulanter på råoljeemulsjonstabilitet med en mikrofluidisk metode; Universal Microfluidic Platform-apparatet. Dessuten å utvikle en metode for dynamisk endring av flokkulant konsentrasjonen i mikrofluidoppsettet. I tillegg har forskjellige metodologier for flokkulant- og emulsjons-karakterisering er blitt utført. Disse inkluderte målinger av størrelse, zeta-potensial og overflatespenning av flokkulantløsninger, og zeta-potensial, overflatepenning og reologimålinger av råoljeemulsjoner. Dessuten ble turbiditeten av råoljeemulsjoner målt over tid for å verifisere resultatene fra mikrofluidmetoden. Arbeidet er en fortsettelse av arbeidet som ble utført i emnet 'TKP4180 - Kjemisk prosessteknologi, fordypningsprosjekt', høsten 2019.

En råolje, fra norsk sokkel, ble brukt til å fremstille emulsjonene. Råoljeemulsjonene ble undersøkt med og uten tilsetning av åtte ulike kommersielle flokkulanter. Studiene viste at egenskaper som størrelse og zeta-potensial for flokkulantene spiller en rolle i emulsjonsstabiliteten. Tilsetningen av flokkulanter til råoljeemulsjonene påvirket også overflatespenningen og reologien. Fra eksperimentene som ble utført med mikrofluidteknikken ble det funnet at resultatene til en viss grad tilsvarer turbiditetsmålingene. En dynamisk endring av flokkulant konsentrasjonen gjorde det også mindre tidkrevende å utføre flere tester, med sammenlignbare resultater.

Det konkluderes med at mikrofluidteknikken er et godt alternativ for undersøkelse av emulsjonstabilitet og en dynamisk endring i flokkulant konsentrasjonen er en tilfredsstillende og tidseffektiv metode for å utføre eksperimenter med mikrofluidteknikken.

Contents

List of Figures

List of Tables

List of Symbols

List of Symbols.

Symbol	Description	Unit
a	Particle radius	m
A	Area	m^2
A_0	Equilibrium Area	m^2
A_a	Area amplitude	m^2
E	Electric field strength	N
$E'(\omega)$	Interfacial dilational elasticity	mN/m
$E''(\omega)$	Interfacial dilational viscosity	smN/m
D	Diffusion coefficient	m^2/s
k_B	Boltzmanns constant	J/K
$f(\kappa a)$	Henry's function	-
g	Gravity constant	m/s^2
l	Mean free path	m
P	Pressure	Pa
P_0	Hydrostatic pressure	Pa
P_{max}	Maximum pressure	Pa
R, r	Radius of curvature	m
R_S	Radius of sphere	m
t	Time	s
T	Temperature	K
Tr	Transmission	%
$Tr_{initial}$	Initial transmission	%
Tr_{final}	Final transmission	%
U_E	Electrophoretic mobility	$m^2/(V{\cdot}s)$
v	Velocity	m/s
v_P	Velocity of particle	m/s
z	Zeta potential	mV

z_v	Vertical distance	m
δ	Phase angle	radian
ε	Dielectric constant	F/m
η	Viscosity	mPa·s
γ	Interfacial tension	mN/m
γ_0	Equilibrium interfacial tension	mN/m
γ_a	Tension amplitude	mN/m
κ	Debye-Hückel parameter	1/m
ω	Angular frequency	radian/s
ρ	Density	kg/m^3
ρ_1	Density of continuous phase	g/cm^3
ρ_2	Density of dispersed phase	g/cm^3
σ	Surface tension	mN/m
Θ	Phase angle	radian

List of Abbreviations

List of Abbreviations.

Acronym	Description
BTEX	Benzene, Toluene, Ethylbenzene and Xylene
CCD	Charge-Coupled Device
CFU	Compact Flotation Unit
DGF	Dissolved Gas Floatation
EIF	Environmental Impact Factor
EOR	Enhanced Oil Recovery
FPSO	Floating, Production, Storage and Offloading
DLS	Dynamic Light Scattering
HOCNF	Harmonized Offshore Chemicals Notification Format
IFT	Interfacial Tension
IGF	Induced Gas Flotation
LDV	Laser Doppler Velocimetry
MLS	Multiple Light Scattering
MQ	Milli-Q
NCS	Norwegian Continental Shelf
ND	Not Determined
NFS	Nutshell Filter
NGL	Natural Gas Liquid
LOC	Lab-On-Chip
PAH	Polycyclic Aromatic Hydrocarbons
PAT	Profile Analysis Tensiometer
PDI	Polydispersity Index
PLONOR	Pose Little or No Risk to the Environment
PWT	Produced Water Treatment
PWRI	Produced Water Reinjection
o/w	Oil-in-water

o/w/o	Oil-in-water-in-oil
SMLS	Static Multiple Light Scattering
TAN	Total Acid Number
TBN	Total Base Number
UMP	Universal Microfluidic Platform
w/o	Water-in-oil
w/o/w	Water-in-oil-in-water

1 Introduction

A important by-product from the production of crude oil is produced water. Several components, including dispersed oil, are present in the produced water. There are several ways to dispose of produced water, for example by discharge directly into the ocean or by re-injection to a reservoir. Before the water can be disposed of, it needs to be treated, and the dispersed oil needs to be removed to be able to meet the requirements for discharges. The treatment of the produced water usually consists of several steps, including gravity separators, hydrocyclones, flotation units as well as membrane treatment.

The phenomena of flocculation and coalescence are desirable during the treatment of the produced water, as these phenomena lead to increased sizes of the oil droplets. Larger droplets will rise faster than smaller droplets, which can improve the separation efficiency. Flocculants, one type of production chemicals, can be added to the produced water to promote the phenomena of flocculation and coalescence. These chemicals can be added to the produced water during the treatment, and are usually added up stream hydrocyclones and flotation units.

The objective of this project is: 1) to study the effect of flocculation and coalescence on oil droplets in water by the use of a microfluidic method, and 2) to develop a procedure to dynamically change the flocculant concentration in the microfluidic setup. The method of microfluidics can be used to control fluids in channels of micro-size and makes it possible to observe and investigate the phenomena of flocculation and coalescence. Nowadays, the most common way to investigate the effect of flocculants have been by the conventional bottle testing [1], where direct observation of the flocculation coalescence has been difficult. Also, additional methods for flocculant and emulsion characterization, as well as emulsion stability, were performed to complement the results from the microfluidics. Namely by the use of the apparatus Zetasizer (Malvern Zetasizer Nano), Maximum Bubble Pressure Tensiometer (BP100), Pendant Drop Tensiometer (Sinterface PAT-1) and Turbiscan LAB.

The experiments were performed at the Department of Chemical Engineering at Ugelstad Laboratory. The project has been a collaboration with the chemical vendor Nouryon.

2 Background

2.1 Crude oil

Crude oil, or petroleum, consists of a mixture of different hydrocarbons in gaseous, liquid and solid form. The composition of the crude oil will vary from field to field, and the oil quality is dependent on, among others, the present hydrocarbons [2]. The crude oil is trapped in permeable and porous reservoir rocks together with formation water and gas caps, and needs to be extracted from the reservoir [3]. The crude oil extraction is defined as recovery and is divided into a primary, secondary and tertiary recovery. Figure 2.1 shows the annual production of oil, condensate, natural gas liquids (NGL) and gas on the Norwegian Continental Shelf (NCS) from the year 1971 to the year 2020.

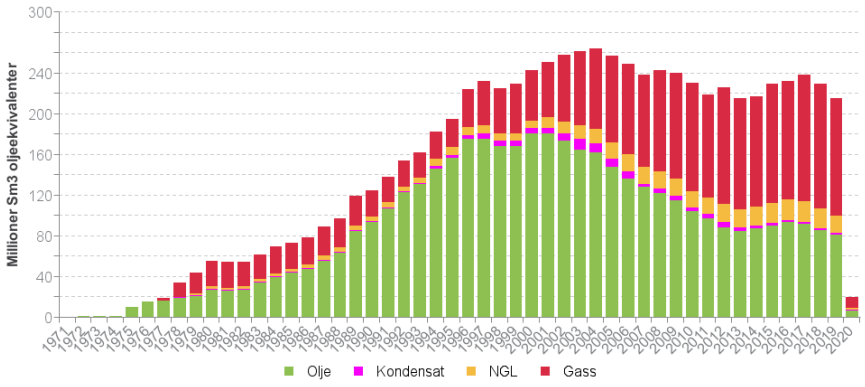

Figure 2.1: Annual production of oil, condensate, NGL and gas on the NCS. Figure is taken from Norsk Petroleum [4].

2.1.1 Crude oil composition

As previously mentioned, crude oil consists of different hydrocarbons in gaseous, liquid and solid form. The hydrocarbons can contain of heteroatomes, for instance, sulphur, oxygen and nitrogen, and metal-organic compounds, as nickel and copper [5]. To ensure flow assurance during the transport of the crude oil, it is essential to characterize the different components in the crude oil. One way to do this is by a SARA separation, where four, extensive constituents in

the crude oil are divided. These four constituents are always present in crude oils and are defined as saturates, aromatics, resins and asphaltenes [6]. During a SARA separation, the saturates, aromatics and resins are separated due to a difference in polarity, while the asphaltenes are separated by a difference in solubility.

The saturates present in the crude oil are non-polar and involve alkanes, both straight and branched, as well as cycloalkanes, without double bonds. This group is typically the lightest group present in the crude oil. Paraffins, which are alkanes with straight chains, are one part of the saturates [7]. Aromatics are molecules often consisting of cycloalkane- and aromatic-rings and alkyl chains, as well as heteroatoms as sulphur and nitrogen. These molecules can be polar. However, molecules with a high molecular weight and high polarity, are usually classified as resins or asphaltenes, instead of aromatics [7]. Resins are polar constituents in crude oil and can often contain heteroatoms like nitrogen, sulphur and oxygen. Asphaltenes also consist of these types of heteroatoms, but in a more significant extent compared to the resins. The most substantial part of metals in crude oil can also be found in the asphaltenes. Besides, the asphaltenes are more polar and have a higher molecular weight than the other constituents in the crude oil, and a lower H/C ratio than the resins. Compared to the resins, the asphaltenes will precipitate in light alkanes, and it is possible to separate them after solubility [7].

2.1.2 Crude oil production

The primary recovery of crude oil, also called natural methods, defines the production of crude oil by driving forces naturally present in the reservoir [8]. The natural mechanisms involved in the primary oil recovery can be, among others, rock and liquid expansion, water drive, gas cap and combination drive, dependent on the reservoir [8]. Secondary oil recovery describes the recovery of oil from the reservoir when the natural mechanisms are no longer sufficient for the production of oil. Processes included in the secondary recovery are usually performed after the primary recovery. However, the secondary recovery can also be performed at the same time as the primary oil recovery [8]. The most common method during secondary oil recovery is water-flooding, where water is injected into the reservoir to maintain or increase the pressure in the reservoir. Injection of gas into the reservoir, called gas-flooding, is also a common method used during secondary oil recovery. Usually, around 10% of the oil in the reservoir is recovered

during primary oil recovery, and around 20-40% of the oil is recovered after both a primary and a secondary recovery [9].

Tertiary oil recovery, also named enhanced oil recovery (EOR), is defined as the recovery of residual oil from the reservoir after the performance of both primary and secondary recovery. Methods used during tertiary oil recovery can be gas- and water-flooding, thermal methods and polymer- and surfactant-flooding, among others [10]. Today, the average recovery factor of oil from the reservoir in Norwegian oil fields are 46% [11]. Although some methods of EOR have been tested in these fields, it is not a method that has been put in action on a field-scale [11].

After the recovery of the crude oil, the fluids from the reservoir usually are separated in a three-phase gravity separator, where the gas, oil and water are separated. Further, the oil can be sent to another gravity separator, typically a two-phase separator, which can contain an electrocoalescer for removal of water from the oil [12]. The reservoir fluids can either be sent to a floating, production, storage and offloading (FPSO) unit, where the oil is recovered, treated and transported, or the oil can be recovered and treated on a platform, before it is transported in pipes or with ships.

2.2 Produced water

In the oil and gas industry, produced water is defined as the water that is produced as crude oil is being extracted from the reservoir. Together with the oil in the reservoir, formation water or natural water will be present, in addition to water that has been injected into the reservoir [13]. Depending on the age, location and depth of the oilfield, the composition of the produced water will vary. Typically, the produced water consists of dissolved inorganic compounds, dispersed oil, dispersed solids, gases, dissolved organics and production chemicals [5].

2.2.1 Produced water composition

Produced water consists of several inorganic ions. These can include sodium, chloride, calcium, magnesium, potassium, sodium and bromide, among others. These ions are also found in seawater. Compared to produced water, the amount of sulphates in seawater is usually higher [14]. Oil in the size of microns is also existing in the produced water. The oil is dispersed due to

the mixing of water and oil, for example, in valves and chokes, when the water is exposed to turbulent flow or pressure drops [5]. There are also many kinds of dispersed solids existing in the produced water, with different origins. For example, the dispersed solids can originate from gas hydrates, the reservoir, scale products, dead microorganisms, corrosion products and can be different precipitation products [5]. Dissolved gases present in the produced water includes O_2, CO_2 and H_2S, which are corrosive gases [14]. Also, hydrocarbons with short chains can be present as gases in the produced water [5]. From data obtained from various oil fields on the Norwegian Sector of the North Sea, the dissolved organics present in the produced water consisted of benzene, toluene, ethylbenzene and xylene (BTEX), polycyclic aromatic hydrocarbons (PAH), phenols and organic acids, among others [15]. Various production chemicals can also be present in the produced water, as they are added to, for example, improve the separation of the produced water or to prevent scale inhibition, asphaltene precipitation, deposits of gas hydrates and corrosion. Chemicals added to the produced water with the goal to improve the separation can be, for example, flocculants.

2.2.2 Produced water management

Every year, a large amount of produced water is discharged from the 87 oil fields producing on the NCS [4]. The amount of discharged produced water is dependent on the age of the oil field and will, therefore, be different for each field. As time goes, the amount of produced water will increase as the amount of oil and gas decreases. The discharge of produced water was 133 million m^3/year on the NCS in 2018, and the expected discharge in 2019 is 139 million m^3/year [16]. Figure 2.2 shows the discharges and projections of produced water discharges on the NCS from the year 1998 to the year 2023 in million m^3/year.

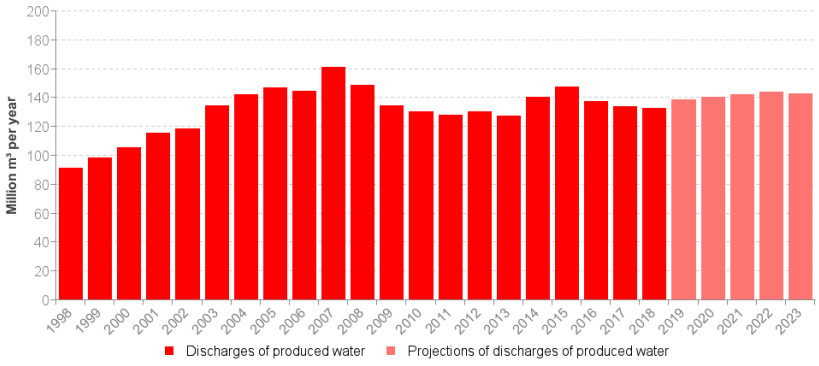

Figure 2.2: Discharges and projections of produced water discharges on the NCS from years 1998-2023. Figure is taken from Norsk Petroleum [4].

To be able to discharge the water, either by produced water reinjection (PWRI) or by discharges directly to the sea, the water needs to be treated to reach the regulations for discharge. When it comes to offshore installations, PWRI is a viable alternative to avoid discharges to the sea [17]. On the NCS, the regulations for discharges of produced water are mainly based on the concentration of dispersed oil and given by the OSPAR Convention, an Oslo-Paris convention made for the protection of the marine environment of the North-East Atlantic [16]. From the OSPAR Convention, the upper limit for the dispersed oil in the produced water is 30 ppm [5, 18]. When it comes to PWRI, the concentration of other components, as dispersed solids, also need to be considered [17]. This is to avoid a formation of, for example, solids and scales, which can decrease the permeability of the formation or cause damage to the equipment [19].

Regarding regulations on production chemicals in the produced water, for example, flocculants and de-emulsifier, an agreement of a zero release of chemicals with harmful risks on the NCS have been made by the Norwegian Parliament [20]. Therefore, an Environmental Impact Factor (EIF), indicating the impact on the environment, have been developed. In addition, the OSPAR Convention have made regulations regarding production chemicals, called Harmonized Offshore Chemicals Notification Format (HOCNF) [20]. This was done to be able to substitute hazardous chemicals with less hazardous products. The regulation demands that there is data available about the given substance, with information regarding bioaccumulation, biodegradability and the aquatic toxicity. Based on data from the HOCNF, production chemicals used offshore in

Norway are classified regarding the acceptance of using them and their effect on the environment. The chemicals ranked after their impact on the environment are characterized as green, yellow, red and black. This ranking is done according to if they are considered to "Pose Little or No Risk to the Environment" (PLONOR), where the PLONOR list is a part of the OSPAR convention [21]. The chemicals characterized as green can be used and discharged, as they are determined to have no or little effect on the environment. The yellow chemicals can also be used and discharged with further specified conditions. The use of chemicals classified as red requires permission from the government before discharged, while the chemicals classified as black can under no circumstances be discharged to the sea [20].

2.2.3 Produced water treatment

The produced water needs to be treated through several steps and in various separation processes before it can be discharged or re-injected to meet the requirements for discharges. Usually, the treatment of produced water is divided and characterised as a primary, secondary and tertiary separation. Before the primary separation step, the produced fluids often has been roughly treated in a three-phase gravity separator, as earlier mentioned. In the gravity separator, water, oil and gas are separated. During the primary separation step, the produced water usually is separated by the difference in density. In this step, it is common to use gravity separators and hydrocyclones. Gravity separators separate the phases by the use of density difference, where the settling velocity of droplets can be described by Stokes law,

$$v = \frac{2R_S^2(\rho_1 - \rho_2)g}{9\eta}. \tag{2.1}$$

Where v is the settling velocity of the droplets, R_S is the radius of the spherical droplets, ρ_1 and ρ_2 are the densities of the continuous and dispersed phase, respectively, g is the gravitational constant and η is the continuous phase's viscosity. From this equation, it is clear that larger droplets will rise faster than smaller droplets. By this principle, gravity separators can separate two and three phases, and they can be both vertically and horizontal. Usually, the gravity separators can separate particles in size range of 100-150 microns [22]. A simple illustration of a horizontal three-phase separator is given in Figure 2.3.

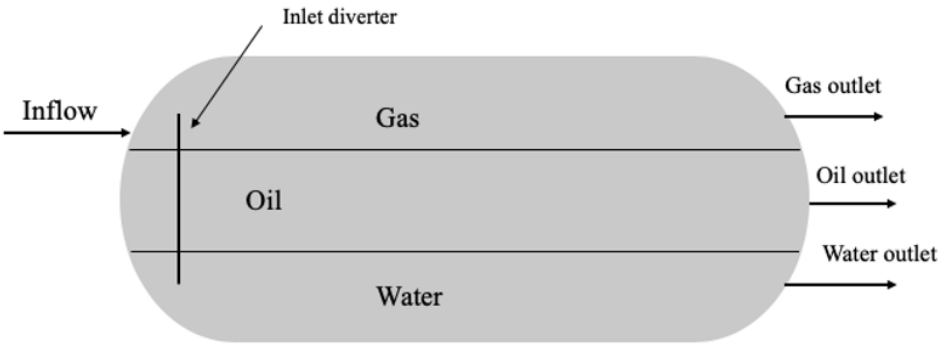

Figure 2.3: Simplified illustration of a horizontal three-phase gravity separator, including an inlet flow and the outlet flows for gas, oil and water.

Hydrocyclones are often used as a part of the primary separation of produced water. They are often used after the water has been treated in gravity separators, as they can separate particles in size range from 10-30 microns [22]. The hydroclyclone separators include an inlet at the top, where the inflow is introduced tangentially. At the top and the bottom of the hydrocyclone, there are exits for the light and the heavy phase, respectively [23]. The working principle in hydrocyclone separators is to separate the different components in the produced water by using a centrifugal force, much larger than the force of gravity. The inflow in the hydrocyclone will experience a spiral motion with direction downward, which will lead the least dense particles to the centre, and the densest particles to the outside [23]. A simple illustration of a vertical hydrocyclone separator is shown in Figure 2.4.

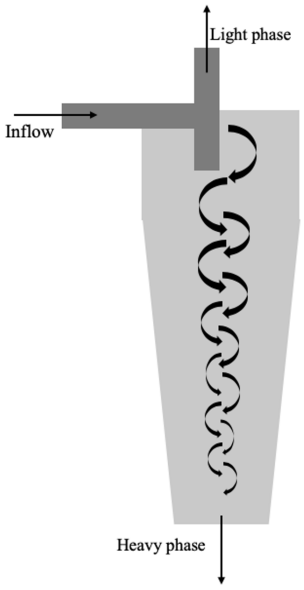

Figure 2.4: Simplified illustration of a hydrocyclone. The illustration shows the tangential inlet at the top, and the outlet for the light phase at the top and outlet for the heavy phase at the bottom.

During the secondary separation step, the use of flotation units is common. The flotation units can be induced gas flotation (IGF), dissolved gas flotation (DGF) and compact gas flotation units (CFU). The separation in the IGF is performed by injection of gas bubbles in size range of 100-1000 microns to the produced water, to remove oil droplets. When a gas bubble and an oil droplet collides, the oil droplet may attach to the gas bubble and rise to the top of the unit faster, according to Stokes law [24]. By the use of IGF's, droplets in the size of 10-15 microns can be removed from the produced water [17]. Figure 2.5 illustrates the principle of attachment of oil droplets to gas bubbles.

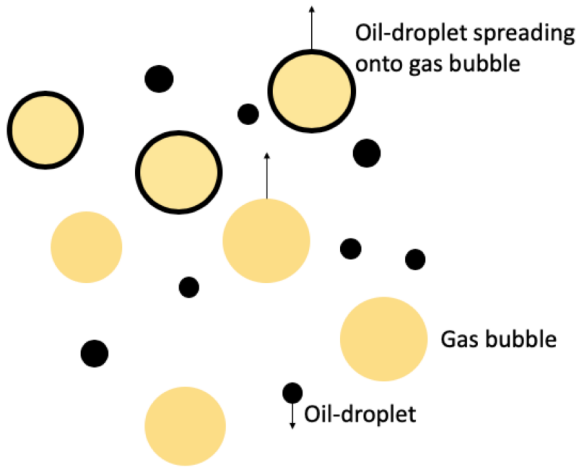

Figure 2.5: Illustration of the separation principle applied in induced gas flotation units, where oil droplets (black) are attached to gas bubbles (yellow).

In the DGF, gas bubbles are produced by manipulation of the pressure of the fluids. The working principle in the DGF is to dissolve the pressurized gas in the liquid phase, and further depressurize it to get the formation of gas bubbles in the size of 10-100 microns [24]. The oil droplets and other solid particles can attach to the microbubbles, and be removed from the liquid phase by the use of a skimmer when reached the surface. The principle for separation by the use of the CFU is both by the introduction of gas to the unit and by providing a centrifugal force. The CFU's can remove particles in size range of 10-15 microns [25]. As the required space for a CFU is normally smaller than for an IGF, it makes it suitable for offshore usage. Several production chemicals, like flocculants, can be added to the produced water to improve the separation by increasing the droplet sizes through promoting the phenomena as coalescence and flocculation. Usually, these chemicals are added to the produced water before the water is treated in hydrocyclones or flotation units. The last step in the produced water treatment, the tertiary separation, can be performed with different types separation technologies. These can be nutshell filters (NFS), and membrane filtration [17], where solids, small oil-droplets and organic compounds are removed before the produced water has reached the requirements for disposal or discharge.

2.3 Emulsion theory

An emulsion is defined as the mixture of two, or more, immiscible liquids, where one is the continuous phase, and the other is the dispersed phase. The dispersed phase makes the droplets, and the continuous phase makes the surrounding liquid. Most emulsions are polydisperse, and the range of droplet-sizes are wide [26]. Different types of emulsions exist; oil-in-water (o/w), water-in-oil (w/o) and multiple emulsions, where water-in-oil and oil-in-water are the two main types of emulsions. An illustration of the two main types of emulsions is given in Figure 2.6. In oil-in-water emulsions, the oil is dispersed in the water, and for water-in-oil emulsions, water is dispersed in the oil. The multiple emulsions can be water-in-oil-in-water (w/o/w) or oil-in-water-in-oil (o/w/o). Oil-field emulsions can be oil-in-water and water-in-oil. The emulsions are formed during the transport and production of crude oil, for example, when the produced water experience turbulent flow in the pipes, or due to mixing across chokes [27].

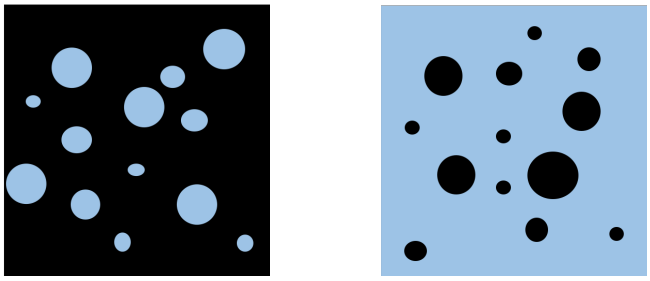

(a) Water-in-oil emulsion.

(b) Oil-in-water emulsion.

Figure 2.6: Illustration of the two main types of emulsions.

2.3.1 Emulsion stabilization

Emulsions, except microemulsions, are kinetically stable, meaning that they will phase separate over time and require the addition of energy to be formed. Dependent on the system, the time it takes to reach phase separation can vary from seconds to years [26]. For oil-in-water emulsions, several mechanisms can stabilize the system. These mechanisms include steric stabilization, electrostatic stabilization, and by low volume fraction of dispersed phase [26].

Steric stabilization occurs as non-ionic macromolecules or solid particles adsorb to the oil-water

interface [28]. The interaction between the macromolecules adsorbed on the oil-water interface leads to an increase in Gibbs free energy when the particles are approaching each other. As a result of this, an arising energy barrier will prevent the distance of the particles from being so small that the van der Waals attractive forces will act dominating [26]. When solid particles have adsorbed to the oil-water interface and formed a stabilizing layer at the interface it is called a Pickering emulsion [29, 30]. The Pickering emulsions is kinetically stabilized by particles with a smaller size than the oil droplets adsorbing to the oil-water interface. An illustration of steric stabilization between two oil-droplets with adsorbed polymer chains and a layer of adsorbed particles are shown in Figure 2.7a and 2.7b, respectively.

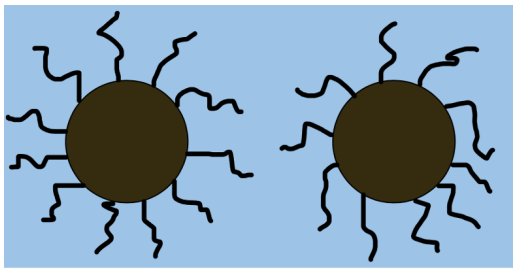

(a) Oil-in-water emulsion stabilized by polymer chains adsorbing to the oil-water interface.

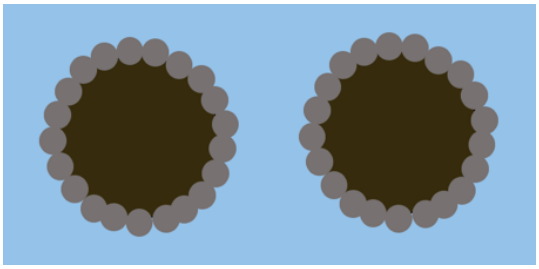

(b) Oil-in-water emulsion stabilized by particles adsorbing to the oil-water interface.

Figure 2.7: Illustration of steric stabilization of oil-in-water emulsions.

Electrostatic stabilization of emulsions occurs when the droplets in the emulsion have the same charge. As a result of this, the droplets will repel each other and stabilize the emulsion. This type of stabilizing mechanism will be most effective when the volume fraction of the particles and ionic strength is low. A low volume fraction of the dispersed phase can also lead to a stable emulsion, as the number of collisions between the particles will reduce, resulting in a decreased coalescence frequency [26]. In produced water, where a high amount of ions are present, this type of stabilization will not be as dominant. An illustration of electrostatic stabilization due to two negatively charged oil-droplets is given in Figure 2.8.

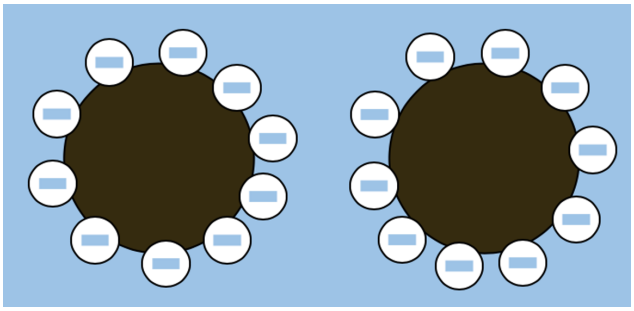

Figure 2.8: Illustration of electrostatic stabilization of two oil-droplets with the same charge.

2.3.2 Emulsion destabilization

In produced water treatment and the separation of oil and water, destabilizing oil-in-water emulsions is essential. There are various mechanisms for destabilizing of oil-in-water emulsions, including sedimentation, creaming, Ostwald ripening, coalescence and flocculation. Sedimentation, a phenomenon that happens when the density of the dispersed phase is larger than that of the density of the continuous phase, results in that the dispersed phase will sediment to the bottom of the emulsion due to gravity forces. Creaming occurs when the density of the dispersed phase is lower than the density of the continuous phase, and the droplets will rise as a result of buoyancy forces. In Ostwald ripening, as a result of mass diffusion, the larger droplets will grow more significant at the expense of the droplets with a smaller size [31]. Coalescence occurs as two, or more, droplets collide and merge to one larger drop, and flocculation describes a reversible formation of particles aggregating and forming "flocs". The mechanisms of coalescence and flocculation will be explained more in detail in Section 2.3.3. An illustration of the mentioned destabilization mechanisms is given in Figure 2.9.

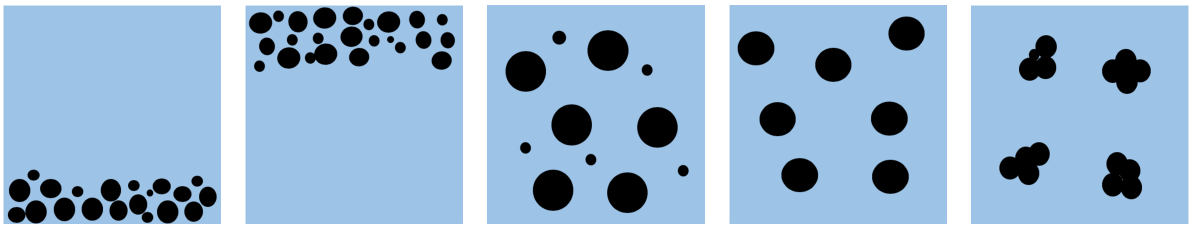

(a) Sedimentation. (b) Creaming. (c) Ostwald ripening. (d) Coalescence. (e) Flocculation.

Figure 2.9: Illustration of destabilization mechanisms for oil-in-water emulsions.

2.3.3 Coalescence and flocculation

Coalescence occurs as two, or more, gas- or liquid-droplets collide and merge to one, larger, droplet [32]. During this mechanism, the droplets involved lose their identity, and the total surface area is reduced [26]. The irreversible process of coalescence can be described by the film drainage model by Shinnar and Church (1960), where three steps explain the process of coalescence [33]. The first step describes the capture of a film of the continuous phase between the particles that are approaching and colliding. The second step describes the drainage of the thin film as it is reaching a critical thickness. Third, and the last step, represents the rupture of the film as it is unstable when it has reached the critical thickness [33]. Figure 2.10 shows the three steps of the process of coalescence. Also, it includes an illustration of the new, larger droplet that is created.

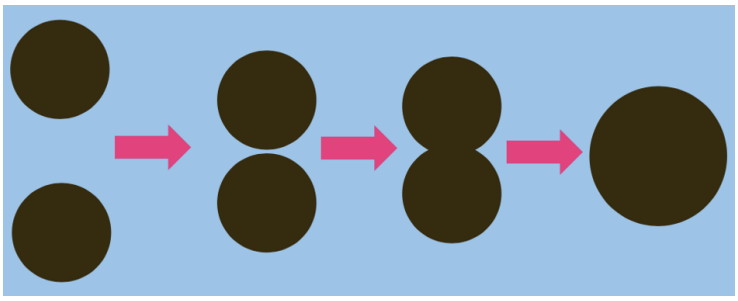

Figure 2.10: Illustration of the different steps in the irreversible process of droplet-droplet coalescence. The first step, from the left, shows the approach of the two droplets. The next step shows the collision of the two droplets, and the third step shows the drainage of the thin film of the continuous phase. The last step shows the new, larger droplet formed during the coalescence process.

Flocculation, as mentioned in Section 2.3.2, is the reversible process of formation of flocs as particles are aggregating. During produced water treatment, flocculants, chemicals that are promoting flocculation, can be added to promote the favourable phenomena as particle aggregation, coalescence and flocculation. The distance between the particles in a floc is significant, which makes the forces between the particles relative small. This makes the flocs to redisperse easily [26]. Flocculants can consist of multivalent ions or polymers, which will act as destabilizing agents. By the use of multivalent ions, the ability to form bindings can be greater, which

can result in flocculation. An example where multivalent cations are used is in the treatment of activated sludge [34].

2.3.4 Flocculation in produced water treatment

In produced water treatment (PWT) it is common to use flocculants which consist of polymers. The polymers used to promote flocculation are usually water-soluble, high molecular weight polyelectrolytes. These can be polycationic, polyanionic, non-ionic or polyamphiphile. In PWT, it is common to use cationic polymers, since the oil droplets usually are negatively charged [26]. Also, cationic flocculants are used in several commercial applications, for example in biotechnology and in the paint and dairy industry where the particles usually have a negative charge [35]. Cationic polymers, compared to non-ionic polymers, are to a lower degree stable and accessible. Non-ionic polymers, which have lower than 1% of charged functional groups and typically have a high molecular weight [35].

The flocculation of particles with the addition of flocculants can happen in two ways; bridging and charge neutralization [35]. The way in which flocculation occurs is dependent on the properties of the particles in the solution and the size of the polymer molecule [35]. The formation of bridges between the particles occurs as the polymer chains adsorb to the particles due to ionic bonds, hydrogen bonds, van der Waals forces or electrostatic attraction [26]. As a result of the bridge formation, the oil droplets can start to flocculate, and further coalesce. For bridge formation between the particles, a high molecular weight is preferred as a longer chain length gives a higher bridge formation [36]. However, a too high amount of flocculants adsorbing to the particles in the solution can give a negative effect, as it can act as a steric stabilizer rather than have a destabilizing effect [26]. A figure illustrating the formation of flocs due to bridging is given in Figure 2.11.

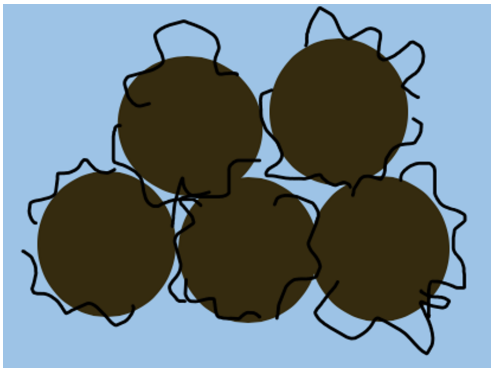

Figure 2.11: Illustration of bridging by polymer adsorbing to the oil-water interface.

Destabilizing of emulsions by charge neutralization can occur when flocculants with opposite charge than the particles are added to the solution. This can cause an attraction, rather than repulsion, between the particles in the solution. Flocculants used in this case often have a lower molecular weight with a high-density charge [36].

Today, the most common way to test the effect of flocculants is by the use of bottle testing (jar tests) [1]. The principle behind the bottle testing is to observe the destabilization of an emulsion over time. Through the addition of flocculants to an emulsion, one can determine the flocculants effect of emulsion destabilization. However, this method can be qualitative as it is dependent on the observation of the samples. Other methods that can be used to examine the effect of flocculants are by multiple light scattering (MLS), or by turbidity measurements.

2.3.5 Surface and interfacial tension

In a system with two phases present, the area at the interface between the phases will be minimized by a contractive force [26]. Interfacial tension, or surface tension, is a measure of this force. The force arises due to an unbalance in the intermolecular forces between the molecules at the interface. These forces acting on the molecules will in total add up to zero for the molecules present in the bulk phase, as they are acting symmetrically on the molecules. The forces will make a thin "film" at the oil-water interface. For the molecules at the surface, the forces acting from the gas phase are negligible, due to the low occupancy of gas molecules. As a result of this, a net attractive force, the surface tension, will act on the molecules at the surface downwards to the bulk phase. For systems where the interface is between two liquids, it is called interfacial

tension (IFT) [26].

As the interfacial tension will try to reduce its area, the spherical shape is the geometry which gives the smallest surface area per unit volume [26]. Therefore, droplets of liquid often have a spherical shape. When it comes to emulsions, a decrease in the interfacial tension could make the emulsions more stable. Therefore, by decreasing the interfacial tension, and at the same time, apply the same energy to the system, there will be a formation of smaller droplets, and hence a more stable emulsion. By the addition of surfactants, surface-active agents, an emulsion can get stabilized.

2.3.6 Interfacial rheology

A measure of the viscosity and elasticity of the interfacial film between two liquids is called interfacial rheology [32]. Both the interfacial viscosity and elasticity can affect the stability of an emulsion. For systems with a high interfacial viscosity, droplet coalescence can more easily occur. This can be explained by that when an interface is applied to stress, there will be an unbalance in the active components adsorbed to the interface. For a system with a high interfacial viscosity, the coalescence between droplets can, therefore, occur before the interfacially active components have been able to return to their place at the interface.

One way to explain interfacial elasticity, is by interfacially active components adsorbing to the oil-water interface and forming a "shell" surrounding the oil-droplets in the emulsion. This surrounding shell will make it harder for the droplets to coalesce when colliding [32].

3 Methodology

During the work on this master thesis, the size, zeta potential and dynamic surface tension of flocculant solutions and the zeta potential, interfacial tension and rheology of emulsions with and without the addition of flocculant were measured experimentally. Also, turbidity experiments were performed to complement the results of the emulsion stability from experiments conducted by a microfluidic setup.

3.1 Size measurements by dynamic light scattering

The Zetasizer was used to measure the size of flocculant solutions by dynamic light scattering (DLS), where it measures the diameter of a sphere that diffuses at an equal velocity as the particle that is being measured [37]. Suspended particles in a fluid will always be moving due to thermal forces, resulting in Brownian motion, a diffusion process. Brownian motion is the motion of particles due to collisions with other particles in the liquid. With DLS, the Brownian motion of the particles suspended in the liquid is determined. The Brownian motion is also dependent on the size of the particles, as larger droplets will move slower than smaller droplets. In the DLS measurements, the particles are illuminated with a laser, and further, the intensity in the light scattered is analysed as it fluctuates over time. The connection between the velocity of the assumed to be spherical particles and their sizes is given in the Stokes-Einstein equation [37],

$$D = \frac{k_B T}{6\pi\eta R}, \tag{3.1}$$

where D is the diffusion coefficient, k_B is the Boltzmann constant, T is the temperature, η is the viscosity of the surrounding liquid and R is the radius of the particle.

3.2 Zeta potential measurements

To measure the charge of particles of flocculants in water and oil droplets in water with and without the addition of flocculants, the Zetasizer apparatus was used. When charged particles are suspended in a solution, the nearby ions will either be repelled or attracted to the particles,

dependent on the charges. The attraction between ions with opposite charge as the particles will lead to a formation of a layer where the ions have adsorbed to the charged particle surface, named the Stern layer. The formation of this layer is due to van der Waals bonds, and or electrostatic bonds [26]. Surrounding the Stern layer, a "cloud" of both co- and counter-ions ions will occur. This cloud of ions is called the Gouy-Chapman layer [26]. The Stern layer, the inner layer, and the Gouy-Chapman layer, the diffuse layer, forms the electrical double layer [26]. As particles in a solution moves, either in an induced or gravitational field or by diffusion, a shear plane will exist outside. Due to this shear plane, the ions present will no longer be affected by the movement of the particles. The zeta potential is defined as the potential at this boundary [32]. An illustration of the Stern layer and the Gouy-Chapman layer is illustrated in Figure 3.1.

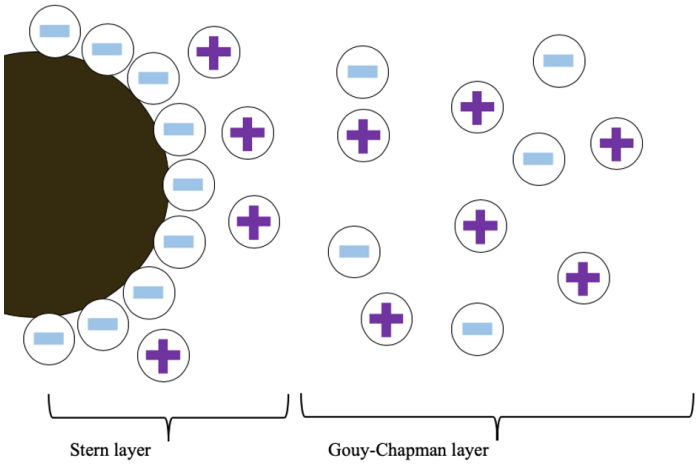

Figure 3.1: Illustration of the Stern and Gouy-Chapman layer, making the electrical double layer.

With the use of laser Doppler velocimetry (LDV), the electrophoretic mobility of the charged particles can be measured by the Zetasizer [32]. The electrophoretic mobility of the charged particles is defined as,

$$U_E = \frac{v_P}{E}, \tag{3.2}$$

where U_E is the electrophoretic mobility, v_P is the linear particle velocity and E is the electric

field strength [26]. With Henry equation, the electrophoretic mobility and the zeta potential can be linked [32],

$$U_E = \frac{2\varepsilon z f(\kappa a)}{3\eta}. \tag{3.3}$$

Where ε is the dielectric constant of the solvent, z is the zeta potential, $f(ka)$ is Henry's function and η is the solvent's viscosity. Included in Henry's function, $f(\kappa a)$, is the thickness of the double layer (Debye-Hückel parameter), κ, and the particle radius, a. If the particle radius is much larger than the thickness of the double layer, the value of 1.5 is used for $f(\kappa a)$, by the Smoluchowski approximation [32, 38].

The value of the measured zeta potential of charged particles in an emulsion can indicate the stability of the emulsion. If the particles suspended in the solution have a high, negative or positive, zeta potential, it will result in particles repelling each other. Due to repelling between the particles, they are not likely to flocculate. For the case of a low absolute value of the zeta potential, the particles are more likely to be attracting each other and further flocculate. As a rule of thumb, a zeta potential of +30 mV, or higher, and a zeta potential of -30 mV, or lower, can indicate a stable emulsion [37].

3.3 Maximum bubble pressure tensiometry

The Maximum Bubble Pressure Tensiometer, BP100, from KRÜSS Scientific makes it possible to experimentally measure the dynamic surface tension as a function of the surface age [39]. The apparatus allows measurements of dynamic surface and interfacial tension, as well as adsorption kinetics, in time scales of milliseconds. The dynamic surface tension is measured with the use of the BP100 by immersing bubbles to a solution through a capillary. As the bubbles are formed, the apparatus detects the maximum pressure. From the values of maximum pressure, the surface tension can be calculated with the Young-Laplace equation, given as,

$$P = \frac{2\sigma}{R}. \tag{3.4}$$

Where P is the internal pressure of a spherical gas bubble, σ is the surface tension, and R is the radius of curvature [39]. The development of a maximum pressure occurs as the curvature of the produced gas bubbles first increases, and then decreases. At the point of the largest

curvature and pressure, the radius of the curvature will be equal to the capillary radius [39]. By performing measurements with a liquid with known surface tension, the radius of the capillary can be determined. Further, when the diameter is determined, the surface tension can be calculated as,

$$\sigma = \frac{(P_{max} - P_0) \cdot R}{2}, \tag{3.5}$$

where P_{max} is the maximum pressure and P_0 is the hydrostatic pressure [39].

3.4 Pendant drop tensiometry

To experimentally determine the IFT and interfacial rheology of liquids, the Sinterface PAT-1 (Profile Analysis Tensiometer) was used.

3.4.1 Interfacial tension measurements

With the use of the Sinterface PAT-1, the shape of a pendant drop can be used to determine the IFT. The relation between the shape of the drop and the IFT is given by the Young-Laplace equation,

$$\Delta P = \gamma(\frac{1}{R_1} + \frac{1}{R_2}), \tag{3.6}$$

where ΔP is the difference in pressure across the drop's interface, γ is the interfacial tension and R_1 and R_2 are the radii of curvature [32]. Since there is no other forces acting on the drop than gravity, the difference in pressure can be expressed as,

$$\Delta P = \Delta P_0 + (\Delta\rho) g z_v. \tag{3.7}$$

Where ΔP_0 is the pressure difference at a reference plane, $\Delta\rho$ is the difference in density, g is the gravity and z_v is the vertical distance between the reference plane and a given point [40]. By combining Equation 3.6 and Equation 3.7 one get,

$$\gamma\Big(\frac{1}{R_1}+\frac{1}{R_2}\Big)=\Delta P_0+\Delta\rho g z_v, \tag{3.8}$$

known as the Gauss-Laplace equation. The Gauss-Laplace equation describes the shape of the drop, and by the use of the coordinates of the drop the IFT can be determined with the Sinterface PAT-1. The device can measure IFT and surface tension in the range of 1-1000 mN/m.

3.4.2 Interfacial rheology measurements

Both the viscosity and elasticity of surfaces and interfaces can be measured during interfacial rheology studies with the Sinterface PAT-1. The interfacial rheology is determined by dilatation, which means that a change in the interface occurs due to applied low-amplitude sinusoidal oscillations to the droplet area. From this, the response of the IFT can be measured [41]. When performing measurements of interfacial rheology with the Sinterface PAT-1, the change in the area of the freshly made oil-droplet upon sinusoidal oscillations can be given as [32],

$$\Delta A = A - A_0 = A_a \cdot sin(\omega t), \tag{3.9}$$

where ΔA is the change in the area, A is the area of the fresh oil-droplet, A_0 is the equilibrium area, A_a is the area amplitude, ω is the angular frequency, and t is the time. During the measurement, the shape of the droplet stays unchanged when the changes in interfacial tension, as the interface tries to re-establish interface equilibrium, is monitored. By axis-symmetric analysis of the shape of the drop, the dynamic interfacial tension is given as [32],

$$\Delta\gamma = \gamma - \gamma_0 = \gamma_a \cdot sin(\omega t + \Theta) \cdot cos\Theta + \gamma_a \cdot cos(\omega t) \cdot sin\Theta. \tag{3.10}$$

Where $\Delta\gamma$ is the change in interfacial tension, γ_a is the tension amplitude, γ_0 is the equilibrium interfacial tension and Θ is the phase angle. The response of a local expansion and compression to an interface can be defined as the interfacial dilational modulus, E, given as,

$$E = \frac{d\gamma}{dlnA}. \tag{3.11}$$

Where $d\gamma$ and $dlnA$ is the change in interfacial tension and area, respectively. The interfacial dilational modulus can be expressed as a complex function [41],

$$E = E'(\omega) + iE''(\omega) = E'(\omega) + i\omega\eta \tag{3.12}$$

where,

$$E'(\omega) = E \cdot cos(\delta), \tag{3.13}$$

$$E''(\omega) = \omega\eta = E \cdot sin(\delta). \tag{3.14}$$

The real part of the function, $E'(\omega)$ represents the interfacial dilational elasticity of the system, the imaginary part, $iE''(\omega)$, represents the interfacial dilational viscosity of the system and δ is the phase angle. As a result of the oscillations applied on the system, the phase angle describes the response from the system. For the case of $\delta = 0°$, the interfacial film is completely elastic, while for the case of $\delta = 90°$, the interfacial film is completely viscous [41].

3.5 Turbidity measurements

To measure the stability of emulsions with and without the addition of flocculants, the Turbiscan Lab apparatus was used. The measurement principle involves measurements of both the transmission and the backscattering from the sample over time. The apparatus consists of a moving detection head, with one detector for transmission and one for backscattering. Also, the detection head consists of an infrared light source. The detector for transmission detects the light that goes through the sample, while the backscattering detector detects the light that gets backscattered by the sample, as the detection head moves up and down over the sample. The principle for measurement in the Turbiscan is static multiple light scattering (SMLS). During SMLS, the detector for backscattering detects the photons which have been scattered multiple times. The photons are scattered by droplets or particles in the sample [42]. The transmission is calculated as,

$$Tr \approx \left(exp(\frac{-r}{l})\right), \tag{3.15}$$

where Tr is the transmission, r is the radius of the particles and l is the mean free path of the photon [43]. The setup also includes temperature control which allows the user to regulate the temperature during the experiments. From these measurements, the stability or instability of an emulsion can be determined over time.

3.6 Microfluidics

One way to investigate emulsion stability and coalescence frequency is by the method of microfluidics, with the Universal Microfluidic Platform (UMP) apparatus. The method of microfluidics is defined as the technology and science where channels in the size of microns are used [44], and it is one method to observe and control fluids behaviour. Microfluidics is a relatively new science, and have been applied in many different fields of science, for example in chemistry, medicine and biology [45]. The improvement of the lab-on-chip (LOC), a device where complete laboratories are integrated into one single chip, has been a great motivation in the research in the field of microfluidics. Channels in micro sizes, pumps, mixers and valves can be integrated into the LOC devices [45]. The chips used in microfluidics can be made out of many different materials, like glass, elastomers, thermoplastics and thermosets.

With the use of the microfluidic technique, there are several advantages compared to an experiment in "regular scale". Due to the channels in the size of microns, the sample volume will be on a small scale. Therefore, the volumes of waste will be on a small scale, which will be both an environmental and an economic advantage [45]. By the use of different chip designs, several aspects with fluid behaviour can be investigated. By changing the chip in the microfluidic setup, it allows the user to reproduce the experiments easy, and reduce the time required to perform several parallels compared to an experiment in a regular scale. Flowrates, pressure and temperature can easily be controlled and adjusted, and experiments can be performed under different conditions. Also, by connecting the microfluidic setup to a microscope and a high-speed camera, the behaviour of the flow in the channels can be observed and analyzed by image analysis.

The technique of microfluidics can also be applied to study the science of emulsions. One advantage by using this technique in the science of emulsions is that it easily allows preparation of monodisperse droplets. The generation of monodisperse droplets can be performed in, for example, a T-junction in the chips [46, 47]. In the T-junction, the dispersed phase and the

continuous phase, from two different channels, will be connected to allow the formation of droplets. Further, the droplet sizes can be changed by adjusting the widths of the channels or the flowrates [47]. The method of microfluidics can be used to investigate droplet-droplet coalescence [48, 49]. Several properties about the droplets and the coalescence can be determined from image analysis, for example, the size and number of droplets in the channel and the coalescence frequency [48].

4 Experimental

4.1 Crude oil

One crude oil from the Norwegian Continental Shelf, denoted as crude oil E, was used during the experiments. For crude oils E, the density, ρ, viscosity, η, total acid number (TAN), total base number (TBN) and SARA fractions of saturates (S), aromatics (Ar), resins (R) and asphaltenes (As) are shown in Table 4.1.

Table 4.1: Properties of crude oil E.

Crude oil	ρ @20°C [g/cm^3]	η @20°C [mPa · s]	TAN [mg KOH/g$_{oil}$]	TBN [mg KOH/g$_{oil}$]	SARA			
					S [%]	Ar [%]	R [%]	As [%]
E	0.831	8.28	0.5	0.4	74.	23.2	1.9	0.1

4.2 Flocculants

In the experiments performed, the effect of eight different commercial flocculants provided by Nouryon and Schlumberger were examined. These are named F1, F2, F3, F4, F5, F6A, F6B and F6C. During the project in the course 'Chemical Engineering, Specialization Project - TKP4580' fall 2019 the effect of F1, F2, F3 and F4 in crude oil emulsions were examined with bottle test and laser diffraction. Therefore, the investigation of F1-F4 is a continuation of the experiments performed fall 2019. F5, F6A, F6B and F6C were provided during the work with this master thesis, where there are some minor differences in the structure between F5 and F6A, and F6B and F6C. F5-F6A where provided with the intention of screening, rather than elaborate testing. Table 4.2 contains the information given about the flocculants, including the classification, pH, amount of solids in per cent and the molecular weight for the flocculants used in the experiments, where "ND" is not determined.

Table 4.2: Properties of F1-F6C.

Flocculant	Classification	pH [-]	Solids [%]	Molecular weight [g/mole]
F1	Polycationic	4.5	6.2	1 000 000
F2	Polyamphiphile	4.0	27.5	100 000
F3	Polycationic	4.5	70	ND
F4	Polyanionic	3.0 - 4.0	-	$>$ 10 000 000
F5	Polycationic (contains hydrophobe)	3.0 - 4.0	-	ND
F6A	Polycationic (contains hydrophobe)	3.6	-	ND
F6B	Polycationic (contains hydrophile)	3.6	-	ND
F6C	Polycationic (contains hydrophile)	3.6	-	ND

During the experiments where flocculants were added, the various flocculant concentrations were achieved by addition of previously prepared concentrated flocculant solutions to the samples. The flocculant solutions were added with a micro-pipette in order to obtain the concentrations required. Compared to the Zetasizer and Turbiscan experiments, where 500 ppm of crude oil were used, the amount of oil in the UMP setup was about 100 times higher. Therefore, the flocculant concentrations needed to account for the higher amount of crude oil was calculated. It was found that a factor of 35 gave an appropriate flocculant concentration compared to the other systems. Therefore, when flocculant concentrations of 10 and 20 ppm are mentioned in this report, the concentrations were, in reality, higher to be able to account for the high water to oil ratio and achieve comparable systems.

4.3 Malvern Zetasizer Nano

4.3.1 Size measurements by dynamic light scattering

For measurements of the size of flocculant particles, a simple, plastic cuvette (3.5 mL) was used. The flocculants, in low-salinity brine (1 g/L), were added to the cuvette and transferred to the Zetasizer where size measurements were performed. In addition, the polydispersity index (PDI) of the flocculant solutions was measured during the size measurements. Concentrations

varying from 20-1000 ppm were investigated to find the lowest concentration of flocculants where both the count rate and PDI had values indicating a stable solution. Each measurement was performed at least two times, with three parallels in each measurement.

4.3.2 Zeta potential measurements

For measurements of the zeta potential for both flocculant solutions and crude oil emulsions with and without the addition of flocculants, a folded capillary cell was used. For the measurements of the zeta potential of flocculants, flocculant concentrations varying from 50-500 ppm in low-salinity brine was added to the folded capillary cell and then immediately transferred to the Zetasizer for measurements. For the emulsions, emulsions of crude oil E (ca. 500 ppm), with and without the addition of flocculants (10 and 20 ppm), were prepared. The crude oil was added to a glass vial, before low-salinity brine was added to the crude oil. Further, the sample was stirred by the use of an Ultra-Turrax, an instrument for high-performance stirring, at 14 000 rpm for one minute. For the samples with the addition of flocculants, the flocculants were added to the emulsions by the use of a micro-pipette. After the emulsion was prepared, it was degassed in a sonic-bath for 30 seconds to remove gas bubbles from the emulsion. Further, the emulsion was transferred to the folded capillary cell and added to the Zetasizer for analysis. In the Zetasizer, three acquisitions for measurements of size and zeta potential were carried out two times at 25 ^{o}C.

4.4 Maximum bubble pressure tensiometry: BP100

Before the dynamic surface tension measurements of flocculant solutions were conducted, the diameter of the capillary, made of glass, was determined with Milli-Q (MQ) water. Further, the dynamic surface tension of the MQ water was measured, to ensure that the system was clean and with no contamination. The MQ water was added to a glass cuvette and placed in the BP100 apparatus. After the glass cuvette was placed in the instrument, the glass capillary was mounted in the BP100. A thermometer was then added into the glass cuvette, and the capillary was brought close to the surface.

After performing measurements with MQ water, solutions of flocculants were examined. The measured capillary diameter was adjusted in the software, and measurements from 10-200000

ms were performed. Flocculants in high-salinity brine (35 g/L) with concentrations varying from 10-1000 ppm were investigated. All of the flocculants were investigated at 1000 ppm, and the flocculants that showed some surface activity were further investigated at 100, 20 and 10 ppm, dependent on if they were surface active. All experiments performed with the BP100 were performed in room temperature ($\sim 22°C$), and each measurement was carried out one time. A figure showing the experimental setup for the BP100 is shown in Figure 4.1. In this picture, the glass capillary is immersed in the liquid in the glass cuvette. The device can be controlled by the control panel shown in the picture.

Figure 4.1: Experimental setup for the BP100.

4.5 Pendant drop tensiometry: Sinterface PAT-1

The setup for the Sinterface PAT-1 consists of two three-way valves, tubing, a cuvette for the sample in a sample cell and a hook for the formation of droplets. Also, the setup includes a computer containing a system for controlled dosing, an adjustable temperature-controlled measuring cell, a CCD-camera (Charge-Coupled Device) consisting of fixed objectives, high-performance frame grabber set up in the PC and cold back-lighting including continuously adjustable intensity [50]. A picture showing the setup for the Sinterface PAT-1 and the software is shown in Figures 4.2a and 4.2b, respectively.

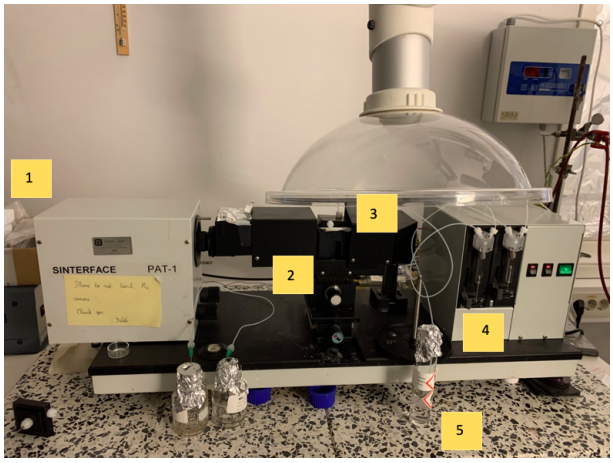

(a) Experimental setup for the Sinterface PAT-1. Number 1 is the camera, number 2 is the cuvette with sample for measurement, including the hook or needle, number 3 is the light source connected to the camera, number 4 is the syringes connected to tubing and three-way valve and number 5 is the sample of crude oil.

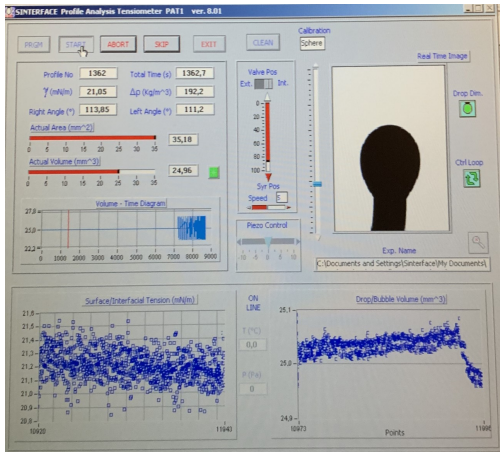

(b) Software used for Sinterface PAT-1, showing the created oil drop and dosing system.

Figure 4.2: Experimental setup for the Sinterface PAT-1 apparatus.

Before performing experiments in the Sinterface PAT-1 small amount of crude oil in a vial was heated up in an oven (60 °C) for approximately 10 minutes. High-salinity brine (20 mL, 35 g/L) was added to the cuvette with a micro-pipette. The heated oil in the vial was connected to the hook by tubing and a three-way valve. The hook was lowered into the NaCl-solution in the cuvette, and the flow of oil was adjusted in the software in the computer to ensure that the volume of the drop had a constant volume of 25 μL during the measurements. A program for measurements of both the dynamic interfacial tension (2 hours) and the measurements of interfacial rheology was performed. The measurements of the interfacial rheology were performed after 2 hours of ageing, with oscillations with a 7% amplitude. This was performed for 5 periods of 100, 80, 60, 40 and 20 seconds. To investigate the effect of the addition of flocculants on the interfacial tension and the interfacial rheology, solutions of flocculants to obtain 20 ppm were added. Two different types of experiments were performed with the addition of flocculants; 1) the flocculant was added in the brine at t=0 seconds and 2) the addition of flocculant at t=2000 seconds, to investigate the effect of ageing. Each measurement was performed at least two times.

4.6 Turbidity measurements: Turbiscan LAB

For the measurements performed in the Turbiscan LAB, emulsions of 500 ppm of crude oil E was prepared. For the sample preparation, oil was weight out in a Schott bottle, and high-salinity brine (35 g/L) was added. Next, the sample was stirred by the use of an Ultra-Turrax. The mixing was performed for three minutes at 10 000 rpm. After the mixing of the sample, it was transferred to a glass-vial used for analysis in the Turbiscan LAB. For the samples with the addition of flocculants, the flocculant was added by the use of a micro-pipette, and the sample was shaken by hand. For the samples without the addition of flocculant, the sample was transferred to the glass-vial and shaken by the hand. Further, the sample was immediately transferred to the Turbiscan LAB for analysis. The measurements were performed every minute for 15 minutes at a temperature of 22^{o}C (room temperature) under static conditions. Concentrations of 10 and 20 ppm of F1, F2, F3 and F4 were investigated with crude oil E. For F5, F6A, F6B and F6C a concentration of 20 ppm were investigated with crude oil E. Each sample was measured three times to obtain reproducibly. Figure 4.3 shows the experimental setup for the Turbiscan LAB, where Figure 4.3a shows the Turbiscan apparatus and Figure 4.3b shows the glass-vial used for sample analysis.

(a) Experimental setup of the Turbiscan LAB instrument.

(b) Glass-vial used for analysis.

Figure 4.3: Experimental setup for the Turbiscan LAB experiments.

For the analysis of the results obtained from the Turbiscan LAB instrument, average values

of the transmission at height 8-12 mm were used. This was used to observe the change in transmission over time at the bottom of the sample. To interpret the results the relative change in transmission, ΔTr, for the samples were calculated as,

$$\Delta Tr = \frac{Tr_{final} - Tr_{initial}}{Tr_{initial}} \cdot 100\%. \tag{4.1}$$

Where Tr_{final} is the final measured transmission and $Tr_{initial}$ is the initial measured transmission.

4.7 Microfluididcs: Universal Microfluidic Platform

Marcin Dudek has developed the procedure for the experimental determination of coalescence frequency by the use of the Universal Microfluidic Platform. The procedure is given in the paper *'Microfluidic tools for studying coalescence of crude oil droplets in produced water'* [51], as a part of his doctoral thesis at NTNU.

The experimental setup for the UMP includes several parts: a high-speed camera (AX100, Photron) connected to an external light source (CoolLED) and an inverted microscope (Ti-U Eclipse, Nikon). Also, it consists of a flow setup (Cetoni Qmix), a chip-holder and chips with micro-channels (Micronit Microtechnologies). Both the inverted microscope and the external light source is connected to the high-speed camera, which makes it possible to see and record the flow inside the micro-channels. The flow setup consist of valves, tubing, pressure sensors, pumps and syringes with different volumes. The flow setup is connected to the chip-holder through tubing. The inverted microscope includes a stage with space for the chip holder. Finally, a computer containing software, namely Qmix Elements for flow-control, and ImageJ for image analysis, is included in the setup. Figure 4.4 shows a picture of the UMP experimental setup.

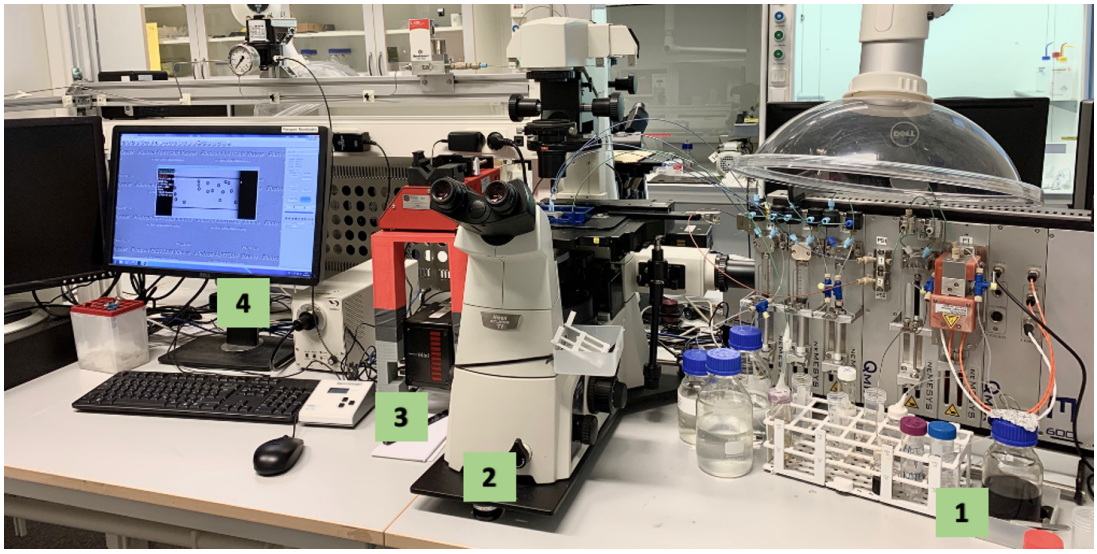

Figure 4.4: Experimental setup for the Universal Microfluidic Platform. Number one shows the flow setup, including pumps, valves, syringes, pressure sensors and tubing. Number two shows the inverted microscope and stage, and the chip-holder. Number three shows the high-speed camera, connected to the external light source and the inverted microscope. Number four shows the computer, including the software for both flow-control and image analysis.

4.7.1 Setup

Firstly, the chip was placed in the chip-holder under the microscope, connected to the high-speed camera and the computer. Further, the syringes were installed in the flow setup, and the tubing was connected to the chip-holder. The syringes used in the experiments were filled with the use of a filling script in the flow-control software. Before each experiment, the crude oil was heated up to approximately 60°C. To get rid of any contamination in the chips, each chip was cleaned in an oxygen plasma chamber before use. During measurements with the UMP, recordings in both the beginning and end of the coalescence chamber were taken. This was done to get a measure of the number and size of the initial droplets and further an estimate on the degree of coalescence. All of the measurements were performed at least three times.

4.7.2 Chip designs

Two different chips, made of glass, were used to investigate the merging of oil droplets in the UMP, with a goal to determine the coalescence frequency of oil droplets and to develop a procedure for a dynamic change of the flocculant concentration in the system. Both chips includes one inlet for the continuous phase and one inlet for the dispersed phase, connected in a T-junction for droplet formation, followed by an ageing channel leading to a wider coalescence chamber. The first chip design consist of an additional inlet at the top of the coalescence chamber, where the flocculant solution, with a set concentration, or brine was added. The second chip made it possible to dynamically change the flocculant concentration, by addition of one additional inlet flow at the bottom of the coalescence chamber. The additional inlet for the additional water phase consisted of two inflows, and were mixed before they reached the coalescence chamber. It also consisted of an extra inlet in the coalescence chamber, which was blocked and not in use. Both chip designs are showed in Figure 4.5.

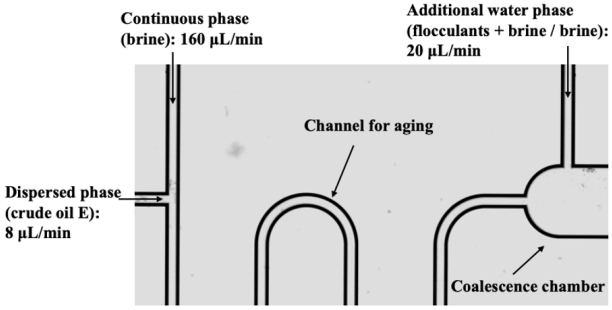

(a) First chip design for investigation of coalescence frequency.

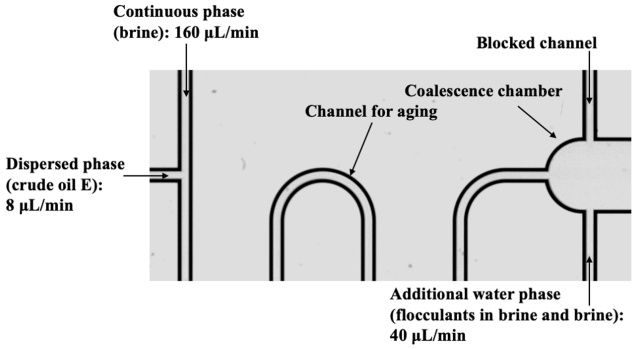

(b) Second chip design used for investigation of coalescence frequency, by a dynamic change of the flocculant concentration

Figure 4.5: Illustration of the two main types of emulsions.

4.7.3 Coalescence frequency experiments

The flows consisted of a continuous phase (high-salinity brine, 35 g/L), a dispersed phase (crude oil E) and an additional water phase. The additional water phase for the first chip design, shown in Figure 4.5a, consisted of pure brine or flocculant in brine with a set concentration to achieve 10 and 20 ppm of flocculants in the system. The additional water phase in the second chip design, shown in Figure 4.5b, consisted of pure high-salinity brine and a flocculant solution in high-salinity brine. The experiments were performed with flows of 160 and 8 μL/min for the continuous phase and dispersed phase, respectively. The additional water phase in the first chip design had a flow of 20 μL/min, while the total flow for the additional water phase in the second chip was 40 μL/min. To dynamically change the concentration of flocculants in the second chip design, the additional continuous phase with a flocculant solution was set to be 0, 10, 20, 30

and 40 μL/min to obtain flocculant concentrations of 0, 5, 10, 15 and 20 ppm, respectively. The brine solution in the additional continuous phase was adjusted according to the flocculant solution flow, to ensure that the total flow of the additional continuous phase flow was always 40 μL/min. 1-1.5 seconds of recordings with a frame rate of 8500 frames per second were recorded during the measurements.

4.7.4 Cleaning of equipment

After the experiments were conducted, cleaning of syringes and tubing were carried out with the use of a script in the Qmix Elements software. Cleaning of the chips included four different solvents (toluene/acetone (3:1), surfactant solution (Decon 90), isopropanol and MQ water). For each solvent, the chips were cleaned for 15 minutes in an ultrasonic bath. After the treatment in the ultrasonic bath, the chips were transferred to a furnace for six hours at 450°C.

4.7.5 Image analysis

After experiments performed in the UMP, the recorded images were analysed and processed to get an exact value of the coalescence frequency of the droplets. The recordings were processed in the image analysis software ImageJ. The processing of the recordings included converting images to binary before the coordinates of the droplet centre of mass and coordinates were transferred to Microsoft Excel. In Microsoft Excel, the coalescence frequency was determined by the use of a developed template [51]. Figure 4.6 shows the original photo converted to binary image and the detected droplets, as well as an output graph from the template including the number of calculated droplets vs number of coalescence events.

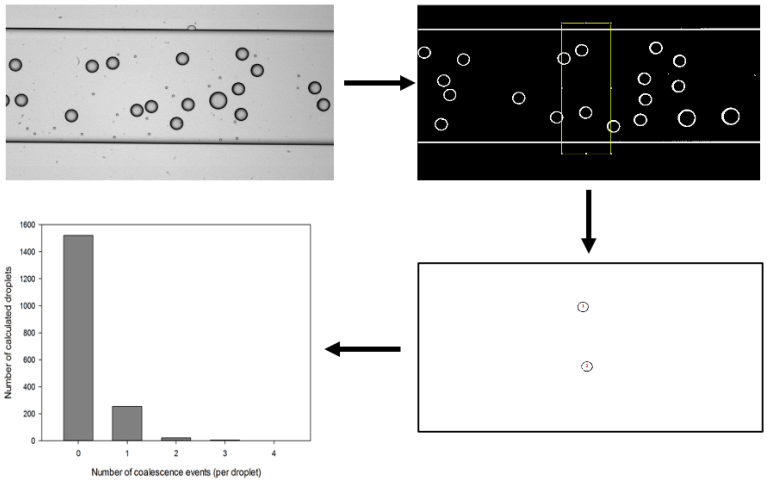

Figure 4.6: Steps of image analysis.

5 Results and Discussion

During the course 'TKP4580 - Chemical Engineering, Specialization Project' fall 2019, bottle tests were performed to investigate the effect of flocculants on crude oil emulsions. In addition, the droplet sizes of emulsions with and without the addition of F1-F4 at 10 and 20 ppm were measured over time. This was performed by laser diffraction with the Malvern Mastersizer 3000 apparatus. These results will be presented and compared with this projects work in Figure 5.14 in Section 5.3.3.

5.1 Flocculant characterization

The flocculant characterization includes size and zeta potential measurements of solutions of flocculants, and a screening of dynamic surface tension of flocculant solutions at various concentrations.

5.1.1 Size and zeta potential measurements of flocculant solutions

The size and zeta potential of solutions of flocculants F1-F6A were measured by the use of the Zetasizer. For F1-F5, solutions of 200 ppm were measured, while solutions of 500, 50 and 300 ppm were measured for F6A, F6B and F6C, respectively. The reason for the different concentrations was to obtain stable solutions of the flocculants, where no aggregation or sedimentation occurred during the measurement. The measured size and zeta potential of the flocculant solutions are given in Figure 5.1 and Figure 5.2, respectively.

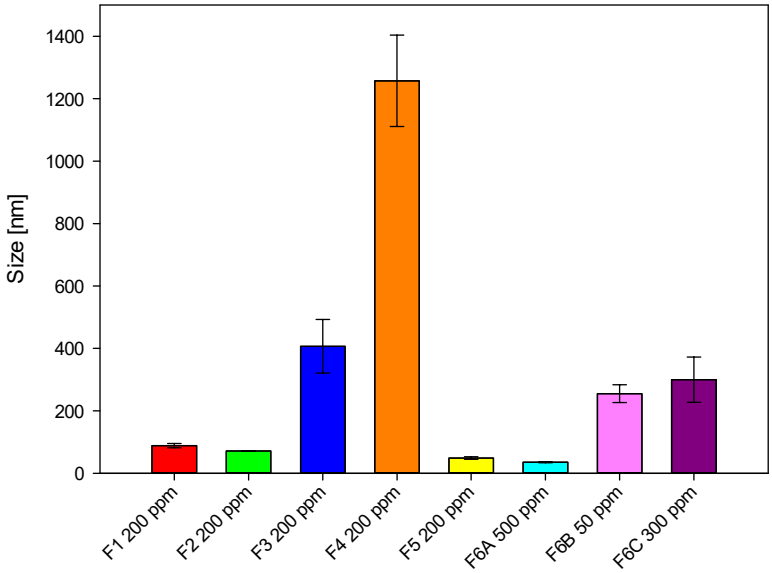

Figure 5.1: Size of solutions of F1-F6C.

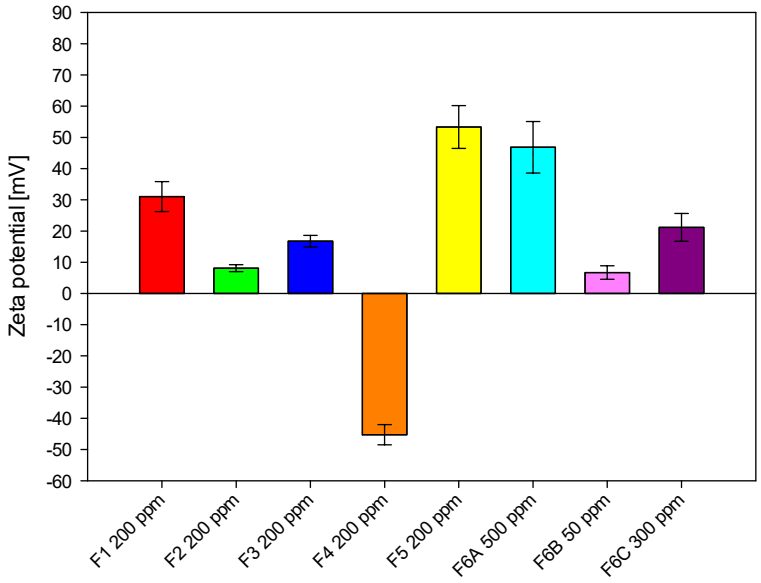

Figure 5.2: Zeta potential of solutions of flocculants F1-F6C.

From Figure 5.1, it can be seen that the particles in the solution of F4 had the largest size, while

the particles in the solution of F6A had the smallest size. For F1, F2 and F4 the measured sizes correspond to the given molecular weights given in Table 4.2 in Section 4.2, where F4 has the largest molecular weight, followed by F1 and then F2. Based on the given properties for the flocculants and the measured sizes, it can be indicated that F5 and F6A have a molecular weight of less than 100 000 g/mole and that F3, F6B and F6C have molecular weights that are, probably, larger than 1 000 000 g/mole.

During the size measurements of the flocculant solutions, the PDI was also measured. The measured values for the PDI is given in Figure A.1 in Appendix A.1. For solutions of polymers, the PDI should have a value around 0.2. However, for all of the flocculant solutions, except F1 and F6A, the measured PDI had considerable higher values. From this, it can be indicated that the flocculant solutions were not completely monodisperse. This, in addition to information about the size distribution by intensity, indicates that F3, F5, F6B and F6C may be mixtures of multi-components, or that they were self associating during the measurements. For F3, F5, F6B and F6C the graphs presenting the size distribution by intensity clearly show several peaks in different size ranges. The graphs presenting the size distribution by intensity for the flocculants are given in Figure A.2 in Appendix A.2.

From Figure 5.2, it can be seen that solutions of all the flocculants, except F4, had a positive zeta potential. The measured zeta potential for the solution of F2 had a relatively low positive value, which could confirm that the flocculant is polyamphiphile, corresponding to its classification in Table 4.2 in Section 4.2. The measured zeta potential of all the flocculant solutions corresponds to their classification.

5.1.2 Dynamic surface tension experiments

The dynamic surface tension of solutions of F1-F6A was screened for surface activity with a bubble pressure tensiometer. Firstly, flocculant solutions of 1000 ppm were examined to investigate if any of the flocculants were surface active. Figure 5.3 shows the measured dynamic surface tension vs the surface age for F1-F6A at 1000 ppm. Exact values for the final measurements are given in Table 5.1. The flocculants that showed some surface activity, all except F1 and F3, were examined at 100 ppm. Further, F5 and F6A, which showed surface activity at 100 ppm were also examined at 20 and 10 ppm. The measured dynamic surface tension for flocculant

solutions at 100 ppm are shown in Figure 5.4, and a comparison between the measured dynamic surface tension for F5 at concentrations 1000, 100, 20 and 10 ppm is presented in Figure 5.5. The corresponding graph presenting the measured dynamic surface tension for flocculant solution of F6A, at 1000, 100, 20 and 10 ppm is given in Figure B.1 in Appendix B.1.

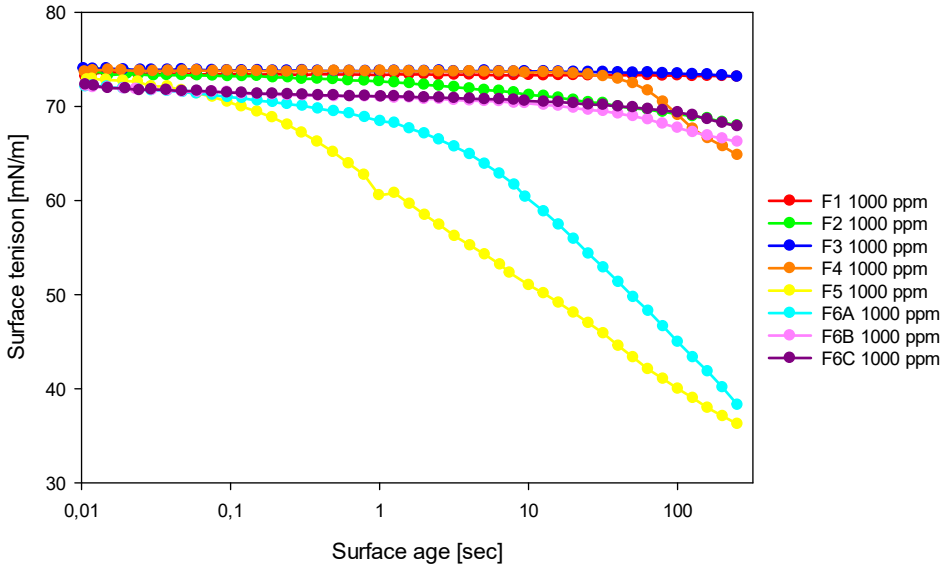

Figure 5.3: Dynamic surface tension vs surface age for solutions of F1-F6C at 1000 ppm. The x-axis shows the surface age, in seconds, plotted on a logarithmic scale.

Table 5.1: Exact values for the dynamic surface tension for the final measurement of solutions of F1-F6C at 1000 ppm.

Sample	Surface tension [mN/m]
F1 1000 ppm	73.2
F2 1000 ppm	68.0
F3 1000 ppm	73.2
F4 1000 ppm	64.8
F5 1000 ppm	35.3
F6A 1000 ppm	38.3
F6B 1000 ppm	66.3
F6C 1000 ppm	67.9

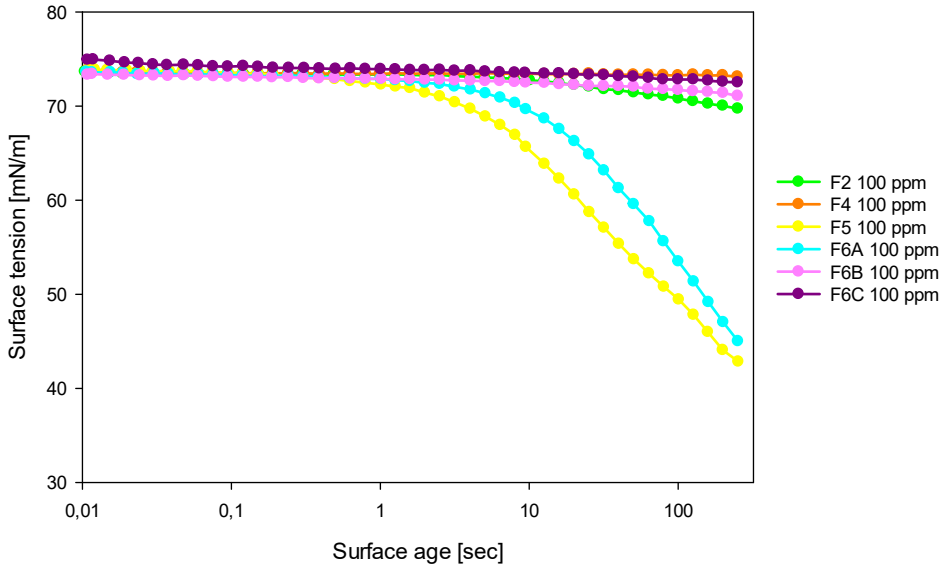

Figure 5.4: Measured dynamic surface tension vs surface age for solutions of F2, F4, F5, F6A, F6B and F6C at 100 ppm. The x-axis shows the surface age, in seconds, plotted on a logarithmic scale.

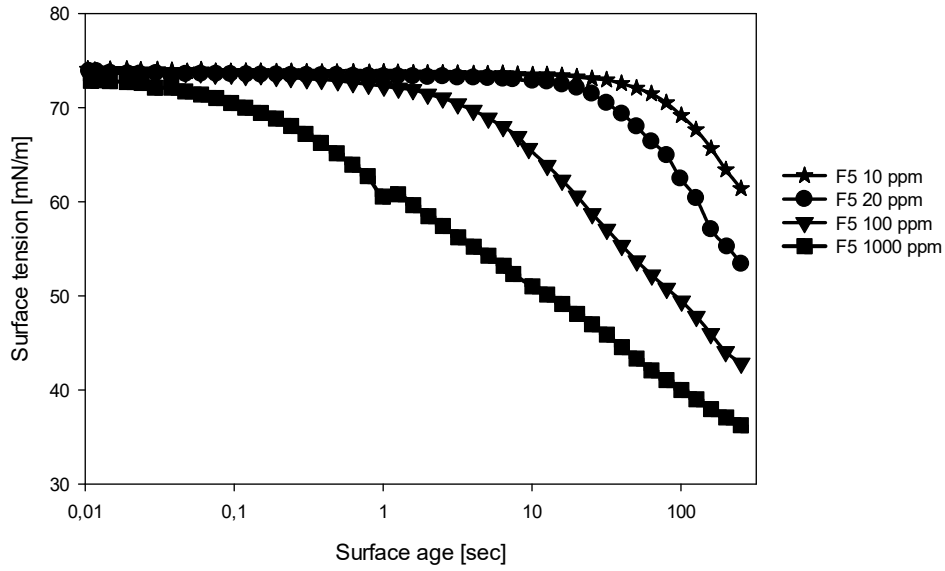

Figure 5.5: Measured dynamic surface tension vs surface age for solutions of F5 at 1000, 100, 20 and 10 ppm. The surface age on the x-axis is plotted on a logarithmic scale.

From Figure 5.3 and Table 5.1, it can be seen that F5 and F6A were highly surface active at 1000 ppm. Also, it can be seen that F2, F4, F6B and F6C showed some affinity to the air-water surface, while F1 and F3 did not show any surface activity within the time of the experiment. From the kinetics observed in Figure 5.3, it could also be deduced that the size of F2, F5 and F6A are small due to a fast decrease in the dynamic surface tension, which corresponds to the results in Figure 5.1 in Section 5.1.1. This could mean that the surface active components have diffused fast to the surface. For F4, the decrease in the dynamic surface tension happened at a later time compared to the other flocculants, and it may be argued that it is due to a larger particle size and its high molecular weight. Also, since the water-air surface is negatively charged, and F4 is an anionic flocculant, the late decrease in the dynamic surface tension may be due to repelling forces between the negative charges. However, it could seem like the surface active components in F4 overcame the repelling forces, since the decrease in the dynamic surface tension occurred at the largest measurement times. Also, since the experiments were performed with flocculants dissolved in high-salinity brine, the effect of the charges may not be significant. These results correspond to the size measurement results obtained from the Zetasizer, given in Figure 5.1 in Section 5.1.1. Also, it can seem like the absolute value of the zeta potential may be a factor in the case of the dynamic surface tension and how it decreases. It can be seen that F4, F5 and F6A have the most significant measured absolute value of the zeta potential, given in Figure 5.2 in Section 5.1.1, and the inclination of the curves in Figure 5.3 appears to follow the same trend.

From Figure 5.4 it can be seen that F2, F4, F6B and F6C did not show any significant surface activity at a concentration of 100 ppm, compared to F5 and F6A. Therefore, solutions of F5 and F6A were examined at both 10 and 20 ppm to investigate if they were also surface active at lower concentrations. From the kinetics observed in Figure 5.5 it can be seen that the curves show a similar trend for all of the concentrations. However, it appears that the decrease in the dynamic surface tension happens faster with a higher flocculant concentration. This could be expected, since a higher flocculant concentration yields a higher number of surface active components, resulting in a greater amount of surface active components at the surface. Hence, a faster change in the dynamic surface tension. The same trend could be seen for the measurements performed with F6A.

5.2 Emulsion characterization

The emulsion characterization measurements includes measurements of the zeta potential of crude oil emulsions with and without flocculants, and interfacial tension and rheology measurements for crude oil with and without addition of flocculants.

5.2.1 Zeta potential measurements of emulsions with and without flocculants

The zeta potential of crude oil emulsions with and without the addition of flocculants was measured with the Zetasizer. Figure 5.6 presents the measured zeta potential for emulsions of crude oil E with and without the addition of F1-F6C at 10 and 20 ppm.

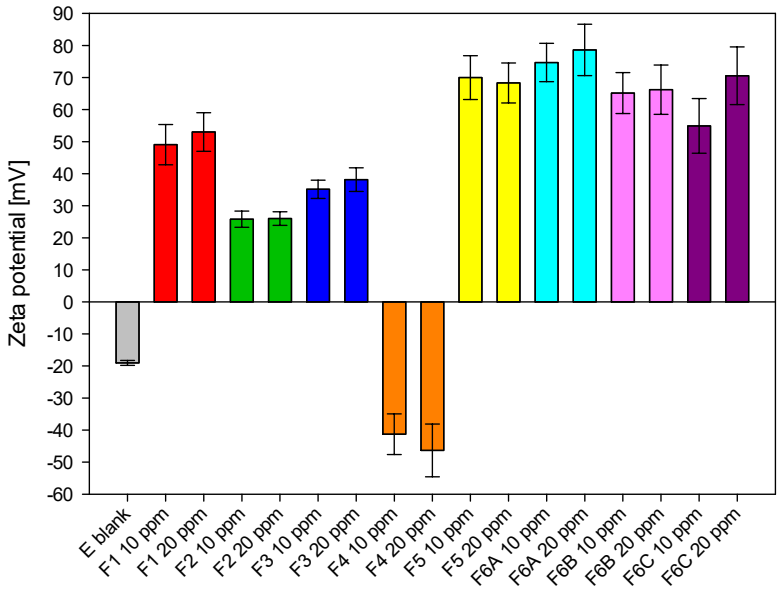

Figure 5.6: Zeta potential for emulsions of crude oil E with and without the addition of F1-F6C at 10 and 20 ppm.

From Figure 5.6, it can be seen that the measured zeta potential for crude oil E without the addition of flocculants was negative, with a value of -19.0 mV. After the addition of all the flocculants, except F4, the zeta potential of the crude oil emulsions became positive, which

is in line with other results [52]. This indicates that the flocculants in these solutions have adsorbed to the oil-water interface and thereby changed the oil droplet charge. It can also be seen that a higher flocculant concentration gave a higher positive zeta potential in almost all of the cases, which can indicate that a higher flocculant concentration yields more adsorption to the oil-water interface. However, the differences in the measured zeta potentials were modest. With the addition of F4 to the crude oil emulsions, the measured zeta potential had a higher negative value compared to the sample with no addition of flocculant. It can, therefore, seem like F4 also adsorbed to the oil-water interface, even though it is an anionic flocculant. As for the other flocculants, also for F4, the value of the measured zeta potential increased, slightly, with increasing flocculant concentration. For all of the emulsions with the addition of flocculants at both 10 and 20 ppm, except for F2, the measured zeta potential had a higher absolute value than 30 mV. Based on the theory [37], this indicates that the emulsions were stable with the addition of flocculants, compared to the emulsion with no addition of flocculants. However, the indication of a stability based on the theory did not correspond to the actual stability in most cases and these results may not be adequate to compare with further emulsion stability measurements, because the emulsions were prepared with low-salinity brine, compared to high-salinity brine in the emulsion stability measurements.

5.2.2 Interfacial tension and rheology measurements

The interfacial tension and interfacial rheology of crude oil E in high-salinity brine with and without the addition of F1-F4 were measured with the Sinterface PAT-1. Figure 5.7 shows the measured interfacial tension as a function of time during two hours of measurement for crude oil E in brine without the addition of flocculants and with the addition of F1-F4 at 20 ppm added at 0 seconds. Figure 5.8 shows the measured interfacial tension for crude oil E in high-salinity brine with and without the addition of F4 at 20 ppm added at 0 and 2000 seconds. The exact values for the measured interfacial tension after two hours, including standard deviations, are given in Table 5.2.

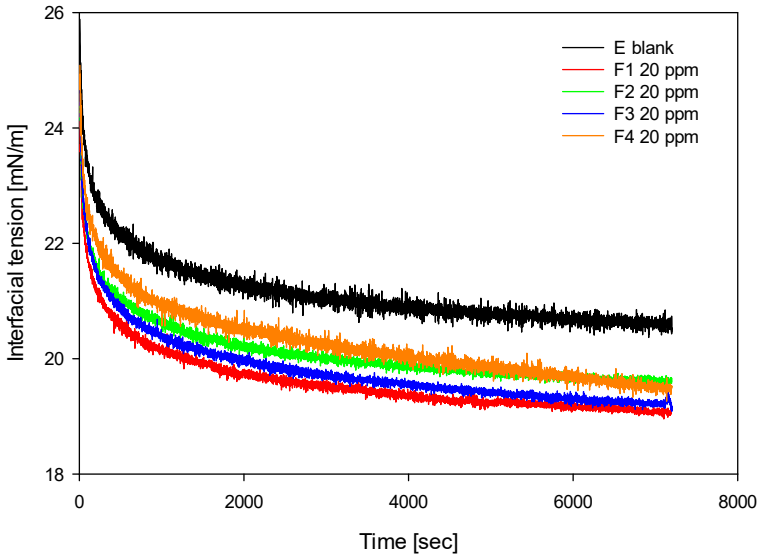

Figure 5.7: Interfacial tension vs time for crude oil E i brine with and without the addition of F1-F4 at 20 ppm added at 0 seconds. The graphs represents an average of the measurements performed.

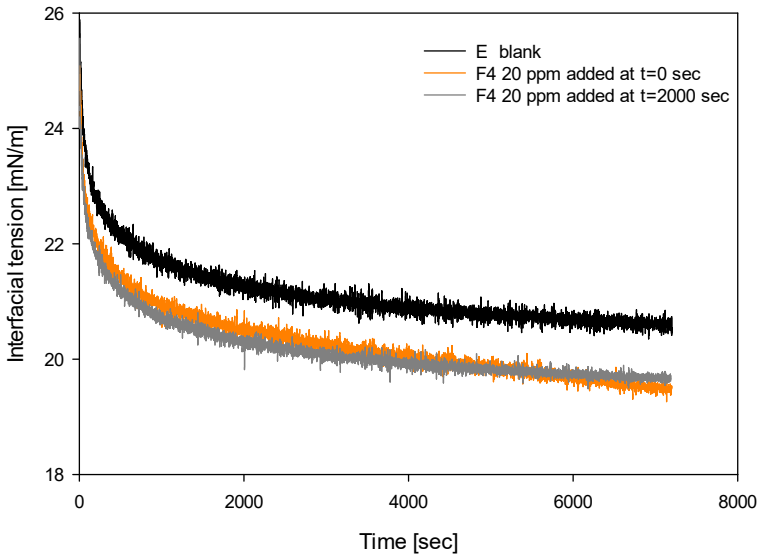

Figure 5.8: Interfacial tension vs time for measurements of crude oil E with and without the addition of F4 at 20 ppm at 0 and 2000 seconds. The graphs represents an average of the measurements performed.

Table 5.2: Exact, average, IFT values after 2 hours, with corresponding standard deviation.

Sample	IFT [mN/m]	Standard deviation [mN/m]
E blank	20.5	± 0.2
F1 20 ppm added at t=0 seconds	19.1	± 0.5
F2 20 ppm added at t=0 seconds	19.6	± 0.4
F3 20 ppm added at t=0 seconds	19.1	± 0.4
F4 20 ppm added at t=0 seconds	19.5	± 0.7
F4 20 ppm added at t=2000 seconds	19.6	± 1.2

From Figure 5.7, it can be seen that the IFT for all the samples decreased from the initial measured value, and approximately obtained a constant value after 2 hours. From the exact values of the IFT, given in Table 5.2, it can be seen that the measured IFT for the samples with the addition of flocculants all reached a slightly lower value compared to the sample without the addition of flocculants. Since the final values of the IFT with the addition of flocculants were similar, it makes it challenging to distinguish between the effect of the different flocculants on the IFT. The decrease in the IFT could be explained by the fact that there have been some interaction between the flocculants and the interface of the crude oil, which was also observed in the zeta potential measurements. To investigate the effect of F4 on the IFT, measurements with pure xylene in brine were performed. This was done to examine if the flocculant showed a change in the IFT in a system with no interfacially active components present. The measured interfacial tension for pure xylene in brine with the addition of F4 after 2000 seconds is shown in Figure C.1 in Appendix C.1. The results obtained from these measurements showed that F4 did not give any change in the IFT, as the value of the IFT had a constant value of around 38-39 mN/m. For that reason, it may seem like F4 is not considerable interfacially active in the case of an oil-water interface. Compared to the results from the BP100, given in Figure 5.3 in Section 5.1.2, where flocculants F2 and F4 gave a small decrease in the dynamic surface tension, it could seem like it is easier for F2 and F4 to adsorb to the surface in the case of an air-water surface, compared to the case of an oil-water interface.

The IFT curves from Figure 5.8 show no significant change in the IFT in the experiments where the flocculant was added after 0 and 2000 seconds. As for the case where the flocculants were

added in the brine at 0 seconds, a small change in the IFT was observed in the case where the flocculant was added after 2000 seconds. However, the standard deviation for the sample with the addition of F4 after 2000 seconds lies in the range of the measured IFT for the sample of crude oil E without the addition of flocculants. In addition, it should be mentioned that the curve of the measured IFT for the sample with addition of F4 after 2000 seconds is similar to the curve where F4 was added at 0 seconds. However, it would be expected that the curve for the case where F4 was added after 2000 seconds should be similar to the sample of crude oil E blank up to 2000 seconds. This might be a result of some contamination in the sample. Therefore, it seems like there is no significant change in the IFT in this case caused by the addition of F4.

After 2 hours of ageing, the interfacial elasticity and viscosity of the samples were determined by performing oscillations on the oil drop. Figure 5.9 shows the measured interfacial elasticity and viscosity for the measurements with the addition of F1-F4 at 20 ppm added after 0 seconds, and for the addition of F4 at 20 ppm after 2000 seconds. The horizontal lines represent the values of the interfacial elasticity and viscosity for the samples of crude oil E without the addition of flocculants.

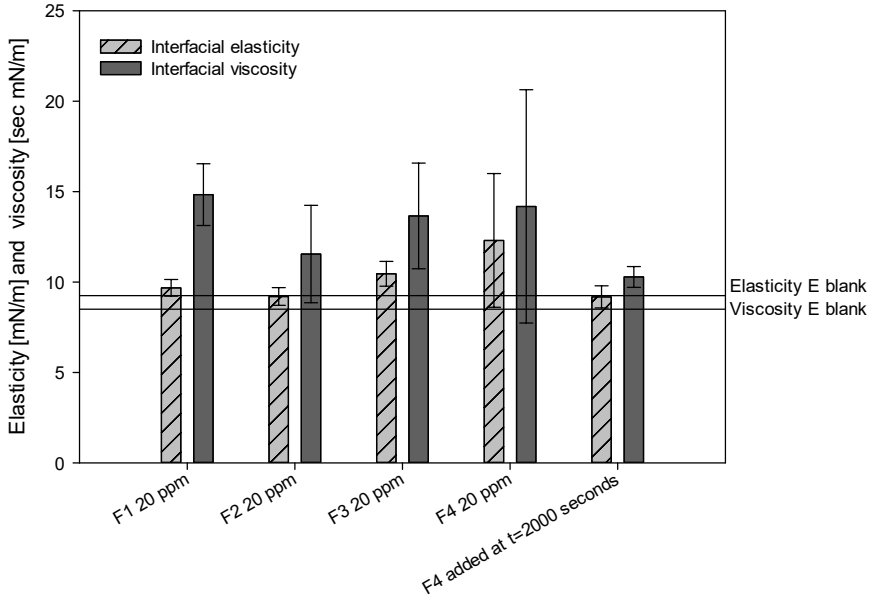

Figure 5.9: Interfacial elasticity and viscosity for crude oil E with the addition of solutions of F1-F4 at 20 ppm after 0 seconds, and solution of F4 at 20 ppm after 2000 seconds.

From Figure 5.9 it can be seen that all for all the samples with the addition of flocculants, an increase in the values for the interfacial viscosity was obtained, compared to the blank samples of crude oil E. Also, the interfacial elasticity increased in the samples with the addition of F1, F3 and F4 added at 0 seconds. Especially for the sample with the addition of F4 at 20 ppm at 0 seconds, it can be seen that there was a significant increase in the measured interfacial rheology parameters. However, the standard deviations are substantial in these measurements. In general, for all the samples where the flocculant was added at 0 seconds, the increase in viscosity was more significant than the increase in the elasticity. For the samples where F4 was added at 2000 seconds, the measured viscosity gave a small increase, while the measured elasticity was approximately the same as for the sample of crude oil E with no addition of flocculants. The great difference in the interfacial elasticity and viscosity between the samples with flocculant F4 could be explained by the fact that the interfacially active components in crude oil would have more time to adsorb to the interface in the case where the interface was aged, and therefore made it harder for the flocculants to interact with or modify the oil-water interface. In the case where the flocculants were added at 0 seconds, the interfacially active components in the flocculant solutions may have been able to adsorb to the oil-water interface before it was "crowded" with crude oil components. It can be argued that an increase in interfacial viscosity could lead to increased coalescence between oil droplets, resulting in a more unstable emulsion. However, for the samples which also achieved an increase in the values for the interfacial elasticity, it could make it harder for the droplets to coalesce, hence a more stable emulsion. For all of the measurements, the interfacial viscosity increased more than the interfacial elasticity after the addition of the flocculants, the opposite as for the sample with no addition of flocculants. This can indicate that the interfaces were more viscous after the addition of the flocculants.

5.3 Emulsion stability

Emulsion stability measurements includes turbidity measurements of emulsions with and without flocculants, and measurements performed with the UMP. Besides, a comparison of the methodologies for emulsion stability measurements. The comparison also includes some of the results obtained from the course 'TKP4580 - Chemical Engineering, Specialization Project' fall 2019.

5.3.1 Measurements of turbidity

The turbidity of emulsions with and without flocculants was measured with the Turbiscan LAB. Figures 5.10 and 5.11 show the relative change in transmission, ΔTr, at the bottom of the sample, at height 8-12 mm, for emulsions of crude oil E with the addition of F1-F4 at 10 ppm and F1-F6C at 20 ppm, respectively. The horizontal lines represent ΔTr for the samples without the addition of flocculants. The values represent the final measurement, after 15 minutes.

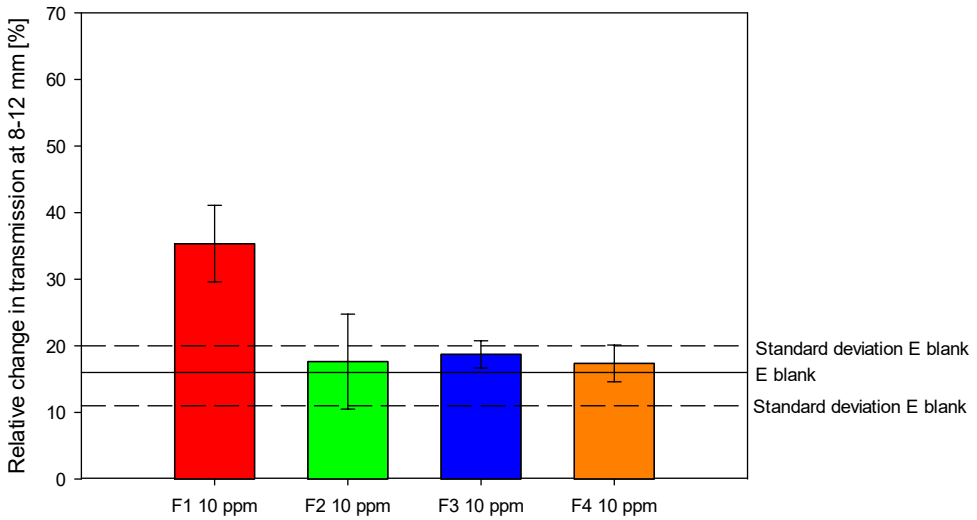

Figure 5.10: Relative change in transmission, given in per cent, for emulsions of crude oil E with the addition of F1-F4 at 10 ppm at height 8-12 mm of the sample after 15 minutes of measurement.

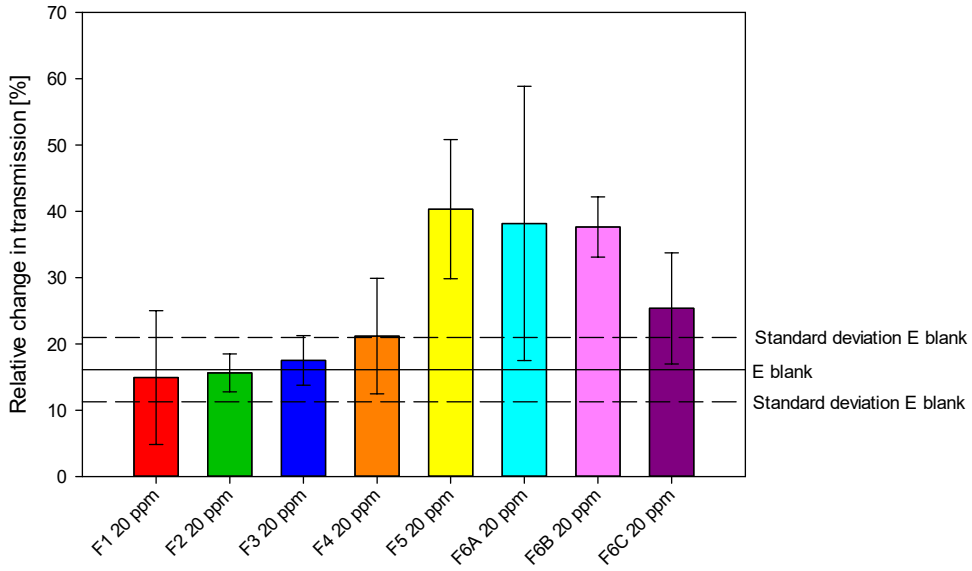

Figure 5.11: Relative change in transmission, given in per cent, for emulsions of crude oil E with the addition of F1-F6C at 20 ppm at height 8-12 mm of the sample after 15 minutes of measurement.

From Figure 5.10 it can be seen that there is a great increase in ΔTr for the emulsions with the addition of F1 at 10 ppm, compared to the sample without the addition of flocculant. A narrow increase in ΔTr can also be observed for F2, F3 and F4. However, the improvement was not considerable, and approximately the same as for the sample without the addition of flocculants. A possible explanation for the large increase in ΔTr with the addition of F1 can be due to the small sizes of the flocculant particles. This could have lead to that the particles diffused faster to the surface, compared to flocculant solutions with larger sizes, as for example, the samples with the addition of F3 and F4. Also, the charge of the flocculants may affect the measured transmission. It can be seen that for F1-F3, which gave positive zeta potentials when added to the crude oil emulsions, the value of ΔTr increased with an increasing value of the zeta potential. This may be explained by that there are larger attractive forces present with a higher positive charge. For the anionic F4, repelling forces between the flocculant particles and the negatively charged air-water surface may have lead to a slower diffusion, and thereby low value of ΔTr in this case.

From Figure 5.11 it can be seen that with the addition of F1 and F2 at 20 ppm, a small decrease in ΔTr was obtained, compared to the case with a lower flocculant concentration. With the addition of F3 at 20 ppm, a modest increase in ΔTr can be observed. With the addition of F4, F5, F6A, F6B and F6C at 20 ppm, a great change in ΔTr were obtained. As mentioned earlier, small particle size may explain the great increase in ΔTr. This may also be the case with the addition of F5 and F6A, where the measured sizes of the flocculant particles were also quite small. For F5-F6C, it appears that the increase in ΔTr approximately decreased with increasing size of the flocculant solutions. These results support the argument that smaller particles could lead to a higher ΔTr in the turbidity measurements. However, this seems not to be the case with the addition of F1 in this case, where the size also was quite small. When it comes to the charge, it can be seen that the flocculants which provided the highest absolute value of the zeta potential in the crude oil emulsions gave the highest increase in ΔTr. Also, F5 and F6A showed a great surface activity of bubbles, which may have contributed to the increase in ΔTr and the diffusion to the surface. In general, F2 and F3 gave the same trend in ΔTr at both 10 and 20 ppm, while F1 gave a lower increase in ΔTr at a higher concentration, and F4 yield a greater increase in ΔTr at a higher concentration.

For the measurements of turbidity, the standard deviations were relatively large for most of the samples. Several different procedures were tested to find a procedure that gave reproducible results from the Turbiscan. One reason for the large deviations could be that the initial samples were not quite the same, which could have affected the results of ΔTr. Due to a small volume of sample and oil used in the Turbiscan, it was challenging to achieve samples with similar initial conditions. One way to avoid these problems could have been to increase the total sample volume. This could have led to a more accurate amount of oil during the weighing of the oil due to a higher amount. However, this would not be environmentally or economically favourable. Also, it may seem like the Turbiscan apparatus was very sensitive to any "noise" on the vials, which may have occurred due to reuse of the vials. To use a new vial every time could have led to a reduction in the standard deviations. However, due to a finite number of vials, this was not possible.

5.3.2 Microfluidic measurements of coalescence frequency

Another way of testing emulsion stability is with the use of the UMP, where the coalescence frequencies of emulsions with crude oil E were determined. Figure 5.12 presents the coalescence frequencies of droplets of crude oil E, with the use of the first chip design, presented in Figure 4.5a in Section 4.7.2. Here, a set concentration of F1-F4 at 10 and 20 ppm was added to the system. The horizontal lines represent the determined coalescence frequency for the sample with no addition of flocculants, with corresponding standard deviations. Figure 5.13 presents the coalescence frequencies for droplets of crude oil E with the addition of F1, F2, F3, F4, F6B and F6C at concentrations of 0-20 ppm. These experiments were performed with the use of the second chip design, presented in Figure 4.5b in Section 4.7.2, where the flocculant concentrations were dynamically changed.

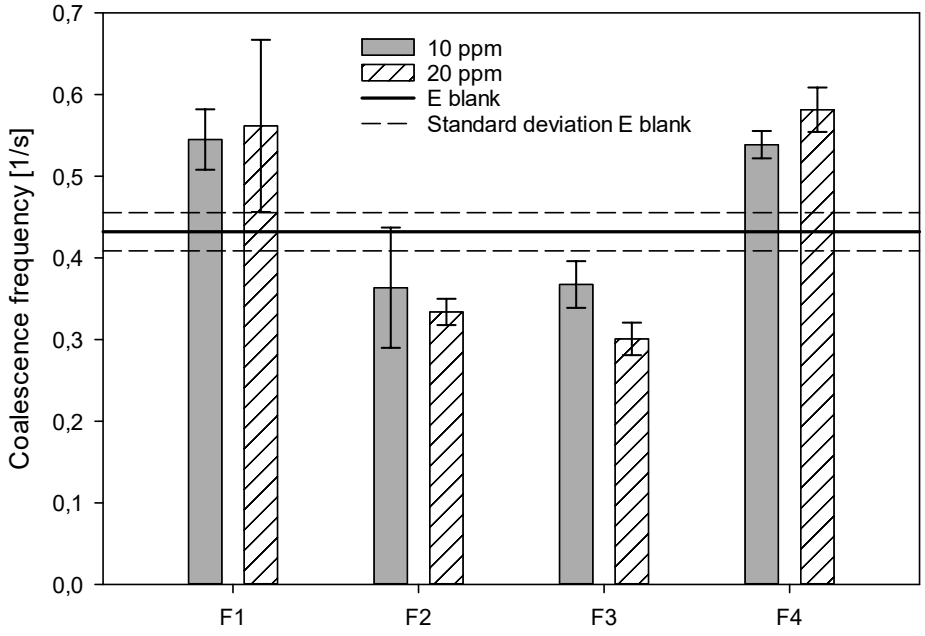

Figure 5.12: Coalescence frequencies for crude oil E with F1-F4 at 10 and 20 ppm. The experiments were performed with the first chip design.

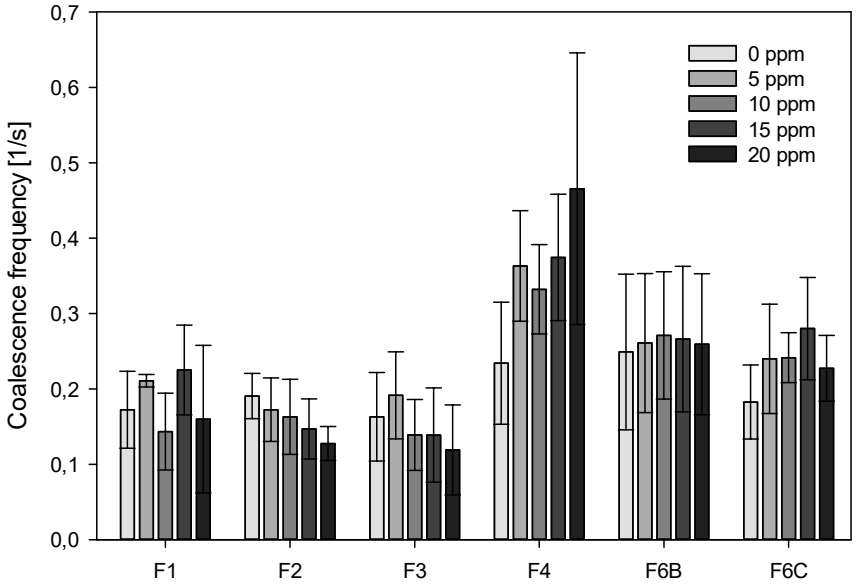

Figure 5.13: Coalescence frequencies for crude oil E with F1-F4 at 0, 5, 10, 15 and 20 ppm 10 and 20 ppm. The experiments were performed with the second chip design.

From Figure 5.12, it can be seen that both F1 and F4 gave an increase in the coalescence frequencies, compared to the sample with no addition of flocculants. For both flocculants, a greater increase in the coalescence frequencies at a concentration of 20 ppm was observed, compared to a concentration of 10 ppm. For F2 and F3, the determined coalescence frequencies were lower than for the sample where no flocculants were added. Also, the coalescence frequencies decreased with an increasing flocculant concentration with the addition of F2 and F3. Therefore, it may seem like F2 and F3, in this case, were dispersing the emulsion, rather than improving merging of the oil droplets.

From Figure 5.13, it appears that the determined coalescence frequencies for F1 were varying, and no clear trend can be seen regarding the different flocculant concentrations. Also, it can be seen that the determined coalescence frequencies for F1 did not correspond to the case where the concentration was set, where the coalescence frequencies increased with an increasing flocculant concentration. However, some problems occurred during measurements of crude oil droplets with the addition of F1. In some cases, the droplets attached to the glass chip, which may have affected the results, and could result in that the results are not ideal to compare

with. For F2 and F3, it can be observed that the determined coalescence frequencies roughly decreased with an increasing flocculant concentration. These results do somewhat correlate to the results obtained when the concentration was set, given in Figure 5.12, where the coalescence frequencies also decreased with an increasing flocculant concentration. For F4, it can be seen that the coalescence frequencies approximately increased with increasing flocculant concentration. Also, the highest total values for the determined coalescence frequencies were obtained for F4. The results obtained with a dynamic change in concentration yield a similar trend compared to the system where the flocculant concentrations were set. It can be argued that the high molecular weight of F4 could play a role in the large increase in the coalescence frequencies in the microfluidic measurements, where there were flow in the system. Since a high molecular weight can increase the number of bridges formed between the particles and the oil droplets, it may be that this is the case for F4, in line with other results [53]. Overall, for F1-F4, the determined coalescence frequencies were higher in the case where the flocculant concentration was set, compared to the case where the concentration was dynamically changed.

From Figure 5.13 it can be seen that F6B gave a narrow increase in the coalescence frequencies with increasing concentration. For F6C, a great increase in the coalescence frequencies were obtained until a flocculant concentration of 15 ppm, where an optimum can be observed. For F5 and F6A, it was not possible to perform experiments in the UMP. When the flocculants were added in the coalescence chamber, they adsorbed to the wall of the chip. Afterwards, the oil droplets adsorbed to the flocculants and it all together stuck to the glass. This attachment may be due to the hydrophobic parts in the flocculants, and the fact that they seemed to be highly surface active. However, it was possible to observe that the oil droplets grew in size and also that the oil droplets attached to the flocculant particles. It can, therefore, be indicated that the flocculants would lead to flocculation or coalescence, even though the experiments were not a success. Snapshots showing the oil droplets adsorbing to the wall of the chip are shown in Figures D.1a and D.1b in Appendix D.1, for F5 and F6A, respectively.

As earlier mentioned, from Figure 5.12 and 5.13, it can be seen that the values of the determined coalescence frequencies were generally lower in the case of measurements with a dynamic change of the concentration. One reason for this could be that the additional water phase had twice the volume flow in the system where the concentration was dynamically changed. With a higher

volume flow, the droplet velocities in the channel would increase. Due to a higher droplet velocity, it could be expected that fewer collisions would take place. The differences in the volume flows may also have affected the droplets in the channel by that the ratio of oil and water was different. A higher oil-water ratio, as in the case of the set flocculant concentration, could be argued to give higher coalescence frequencies, due to a higher oil concentration in the system and larger chance of collisions.

It can be observed that the standard deviations were, generally, higher in the case where the concentrations were dynamically changed, compared to when the concentrations were set. However, the errors for each parallel were not as high as the standard deviations, which may indicate that the parallels were not completely similar, even though the errors for each parallel were satisfactory. Several factors could have affected this. One reason for the large deviations in the case where the concentration was dynamically changed could be due to a late response of the pumping system when the flows were adjusted to change the concentrations. This could have resulted in inaccurate concentrations in the coalescence chamber. Time wise, it was less time consuming to perform several experiments with different concentrations by a dynamic change in the flocculant concentration, compared to when the flocculant concentration was set. In comparison, in the former five concentrations were measured during one test, whereas only one could been tested for the latter method.

5.3.3 Comparison between emulsion stability methodologies

Figure 5.14 presents an overview of the emulsion stability measurements performed with the addition of F1-F4 at 10 and 20 ppm. The results include both the results obtained from the experiments conducted during the work on this project and the results obtained during the work in the course 'TKP4580 - Chemical Engineering, Specialization Project' fall 2019, where bottle tests and light scattering measurements were performed. The graph presents the relative differences compared to the samples with no addition of flocculants in per cent. The microfluidic results presented in the graph are from the measurements with the chip where the flocculant concentration was set, given in Figure 4.5a.

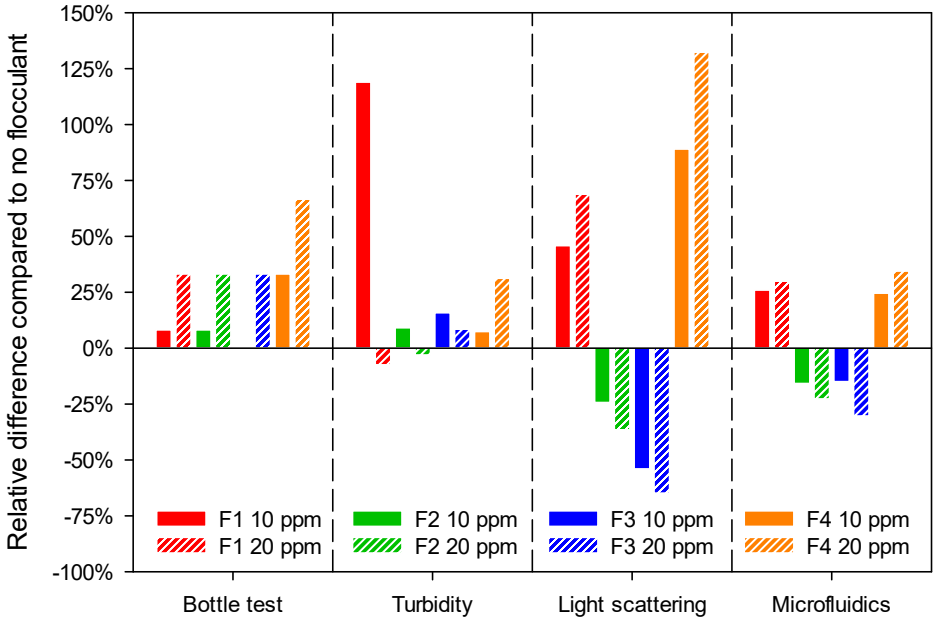

Figure 5.14: Comparison between the different methods used to investigate the emulsion stability by the addition of F1-F4 at 10 and 20 ppm.

From Figure 5.14, it can be seen that the results obtained with the light scattering and the microfluidics correspond and show the same trend regarding all of the flocculants at both concentration 10 and 20 ppm. From these results, F1 and F4 were improving the emulsion destabilization at both 10 and 20 ppm, while F2 and F3 were acting stabilizing. On the other hand, the results from the bottle testing and the turbidity measurements were different regarding F2 and F3 at both 10 and 20 ppm, compared to the light scattering and microfluidic measurements. In the bottle tests, all of the flocculants, except F3 at 10 ppm, destabilized the emulsions, and in the turbidity measurements F1 and F2 at 20 ppm were stabilizing the emulsion. When it comes to F1 and F4, it can seem like they, in general, improved the emulsion destabilization in most of the emulsion stability measurements.

There are several differences between these methods of measurements of the emulsion stability, and there were strengths and weaknesses to every method. Firstly, the bottle tests and turbidity measurements were performed under static conditions. In contrast, the light scattering and microfluidic measurements are performed with a flow during the measurements, which provided different measurement conditions. Compared to a real produced water treatment process, flow

in the measurements would be more similar and comparable.

When it comes to the results regarding the emulsion stability obtained from the different methods, there were also differences. The bottle tests results were based on observation of the destabilization over time. Therefore, these results are qualitative and might be a little inaccurate. The turbidity measurements could give an indication on the emulsion stability, as it provides measurements of the exact transmission through the samples. For the turbidity measurements, the standard deviations were relatively large, and the measured transmission of the samples may have been affected by noise on the glass vials. The obtained transmission from the turbidity measurements could have been affected by this, and some inaccuracy may have occurred. Also, different initial distributions also could have lead to the high standard deviations. During the light scattering measurements, information about different droplet sizes in the emulsions were provided during the entire measurement. However, during the light scattering measurements some creaming of the oil were observed, which could have given a more accurate measure of the smallest droplets, compared to the larger droplets. For the microfluidic measurements, it was possible to get direct observations of the flows in the channels, and from that an exact measure of the coalescence frequencies. This gave a broader image of the droplet distributions in the emulsions, compared to the light scattering measurements where the provided information was about the size distributions kinetics.

Another difference between the methodologies was the amount of sample and waste accumulated in the measurements. In the bottle tests and turbidity measurements, approximately 40 mL of sample was used to prepare each emulsion. For the light scattering experiments, about 500 mL of sample was used for each analysis. Besides, a considerable amount of chemicals were needed for cleaning of the samples in the light scattering measurements. In the microfluidic experiments, each sample required approximately a volume of 1-5 mL, and reduced even further with dynamic change of the flocculant concentration. When it comes to the oil concentrations in the emulsions, an oil concentration of 500 ppm was preferable, since it would be similar to the actual oil content in produced water. For the bottle tests, turbidity measurements, and light scattering measurements the oil concentration in the prepared emulsions were 500 ppm. However, for the turbidity measurements, an oil concentration of higher than 500 ppm was required to get satisfactory measurements, while in the light scattering the upper limit was 500

ppm. This was because higher oil concentrations in the light scattering measurements could lead to multiple scattering which could result in false results. In the microfluidic measurements, the oil concentration was much higher. This may also have made the conditions and measurements different.

Time-wise, there were also several differences. The light scattering measurements clearly stood out, which was the most lengthy emulsion stability method. This was due to a time-consuming cleaning procedure after performed measurements, and each experiment required ca. 60-90 minutes in total. For the bottle tests, each sample required ca. 30-40 minutes. For both the turbidity and microfluidics measurements, each sample took approximately 20-30 minutes. However, the cleaning and start-up processes in the microfluidic took some time, which made the total time for several measurements longer, even though each parallel was relatively fast and the statistics were better.

6 Conclusions and further work

This project aimed to investigate different flocculants effect on crude oil emulsion stability by the use of a microfluidic technique and to develop a procedure to dynamically change the flocculant concentration in the microfluidic setup. In addition, to complement and verify the results from the microfluidic setup by turbidity measurements. Measurements regarding the characterization of the flocculants and crude oil emulsions were also performed. This was done to investigate different properties of the flocculants and complement the emulsion stability measurements.

It was found that the measured sizes of the flocculant solutions correspond to the provided data regarding F1, F2 and F4. Also, the classification of the flocculants corresponds to the measured zeta potentials. When it comes to surface activity, it was found that F1 and F3 were not surface active and that F2, F4, F6B and F6C showed some surface affinity. F5 and F6A showed to be highly surface active. The cationic flocculants turned the zeta potential of the crude oil emulsions from negative to positive, and all of the flocculants increased the absolute value of the zeta potential when added to crude oil emulsions.

During measurements of the interfacial tension of crude oil with and without the addition of flocculants, it was found that the flocculants gave a slight decrease in the interfacial tension. A change in the interfacial rheology parameters was obtained with the addition of F1-F4. However, no correlation between the interfacial rheology properties and the emulsion stability was found.

From the turbidity measurements, performed under static conditions, the size and charge of the flocculant particles play a significant role where the flocculants with the smallest sizes gave the largest increase in the relative change in transmission in many cases. Also, a higher absolute value of the zeta potential of the flocculants yielded a more unstable emulsion.

The results obtained from the microfluidic technique, both with a set and dynamically changed flocculant concentrations, provided similar trends when it comes to the different flocculants effect. However, since the volume flows were not the same, a considerable difference in the values of the coalescence frequencies was obtained. The emulsion stability results obtained from the turbidity measurements and the measurements performed with the microfluidic technique do to some degree compare, by showing the same trends regarding the flocculants effect for some of the flocculants. However, limitations regarding the reproducibility and large deviations obtained

from the turbidity measurements make it challenging to compare the results. From comparison between the results obtained in this project and in 'TKP4580 - Chemical Engineering, Specialization Project' fall 2019, it is concluded that static and dynamic measurement conditions plays a significant role in the correspondences of the results.

In summary, no clear trend regarding the properties of the flocculants shows to be dominant for the effect of the flocculation and coalescence. Overall, from the results obtained during this study regarding the different flocculants effect, it is concluded that F1, F4, F6B and F6C gave an increase in the flocculation and coalescence of the oil droplets in the crude oil emulsions. Also, it is concluded that F2 and F3 were dispersing the emulsions, rather than promoting flocculation and coalescence. For F5 and F6A, more tests should be conducted to get a broader picture of the flocculants effect on the flocculation and coalescence. Ultimately, the microfluidic method is an effective and useful method to investigate the stability of crude oil emulsions, and it was shown to give comparable results to the other emulsion stability measurements. Therefore, it is concluded that it is a good option to the conventional methods for emulsion stability measurements.

Future studies could include bottle tests and light scattering measurements for F5-F6A. Also, it could include measurements of the interfacial tension with the addition of F5-F6C, to observe if they give any change in the interfacial tension of the crude oil. In addition, turbidity measurements performed with a new vial every time could be performed to investigate if this may lead to a reduction in the standard deviations. For the microfluidic measurements, future studies can include further development of the method of a dynamic change in the flocculant concentration by trying to reduce the standard deviations and get more similar parallels. This could be done by making sure that the measurements were performed with no delay in the pumping system. One way could be to, for example, perform the measurements at the same time for each measurement, after exploring the exact response of the pumping system.

References

1. *Polymers for Water and Wastewater Treatment* Library Catalog: tramfloc.com. `http://tramfloc.com/polymers-selection-jar-testing-procedures/` (2020).
2. *Historical production on the NCS* Library Catalog: www.norskpetroleum.no. `https://www.norskpetroleum.no/en/facts/historical-production/` (2020).
3. Guo, B., Lyons, W. C. & Ghalambor, A. in *Petroleum Production Engineering* (eds Guo, B., Lyons, W. C. & Ghalambor, A.) 1 (Gulf Professional Publishing, Burlington, Jan. 2007).
4. *Norwegian Petroleum* `https://www.norskpetroleum.no` (2020).
5. Dudek, M., Vik, E. A., Aanesen, S. V. & Øye, G. Colloid chemistry and experimental techniques for understanding fundamental behaviour of produced water in oil and gas production. *Advances in Colloid and Interface Science* **276,** 102105 (Feb. 2020).
6. Umar, A. A., Saaid, I. B. M., Sulaimon, A. A. & Pilus, R. B. M. A review of petroleum emulsions and recent progress on water-in-crude oil emulsions stabilized by natural surfactants and solids. *Journal of Petroleum Science and Engineering* **165,** 673–690 (June 2018).
7. Muhammad, I. *et al.* SARA Separation and Determination of Concentration Levels of Some Heavy Metals in Organic Fractions of Nigerian Crude Oil. *Chemistry and materials research* **3,** 7–14 (July 2013).
8. Ahmed, T. in *Reservoir Engineering Handbook (Fourth Edition)* (ed Ahmed, T.) 909–1095 (Gulf Professional Publishing, Boston, Jan. 2010). (2020).
9. *Enhanced Oil Recovery* Library Catalog: www.energy.gov. `https://www.energy.gov/fe/science-innovation/oil-gas-research/enhanced-oil-recovery` (2020).
10. Druetta, P., Raffa, P. & Picchioni, F. Chemical enhanced oil recovery and the role of chemical product design. *Applied Energy* **252,** 113480 (Oct. 2019).
11. Pham, V. & Halland, E. Perspective of CO2 for Storage and Enhanced Oil Recovery (EOR) in Norwegian North Sea. *Energy Procedia* **114,** 7042–7046 (July 2017).
12. Nguyen, T.-V. *et al.* Exergetic assessment of energy systems on North Sea oil and gas platforms. *Energy* **62,** 23–36 (Dec. 2013).

13. Igunnu, E. T. & Chen, G. Z. Produced water treatment technologies. *International Journal of Low-Carbon Technologies* **9.** Publisher: Oxford Academic, 157–177 (Sept. 2014).
14. Neff, J., Lee, K. & DeBlois, E. M. in *Produced Water: Environmental Risks and Advances in Mitigation Technologies* (eds Lee, K. & Neff, J.) 3–54 (Springer, 2011).
15. Røe Utvik, T. I. Chemical characterisation of produced water from four offshore oil production platforms in the North Sea. *Chemosphere* **39,** 2593–2606 (Dec. 1999).
16. *Discharges to the sea* `https://www.norskpetroleum.no/en/environment-and-technology/discharges-to-the-sea/` (2020).
17. Judd, S. *et al.* The size and performance of offshore produced water oil-removal technologies for reinjection. *Separation and Purification Technology* **134,** 241–246 (Sept. 2014).
18. Commision, O. *Discharges, Spills and Emissions from Offshore Oil and Gas Installations in 2016*
19. Mackay, E. J., Collins, I. R., Jordan, M. M. & Feasey, N. PWRI: Scale Formation Risk Assessment and Management, 18.
20. Beyer, J. Environmental effects of offshore produced water discharges evaluated for the Barents Sea, 84.
21. *Offshore Chemicals* Library Catalog: www.ospar.org. `https://www.ospar.org/work-areas/oic/chemicals` (2020).
22. Stewart, M. & Arnold, K. in *Produced Water Treatment Field Manual* (eds Stewart, M. & Arnold, K.) 1–134 (Gulf Professional Publishing, Boston, Jan. 2011).
23. *Hydrocyclones - an overview — ScienceDirect Topics* `https://www.sciencedirect.com/topics/materials-science/hydrocyclones` (2020).
24. Saththasivam, J., Loganathan, K. & Sarp, S. An overview of oil–water separation using gas flotation systems. *Chemosphere* **144,** 671–680 (Feb. 2016).
25. *Compact flotation unit cut soil in water to 10-15 ppm* Aug. 2004. `https://www.offshore-mag.com/business-briefs/equipment-engineering/article/16756981/compact-flotation-unit-cut-soil-in-water-to-1015-ppm` (2019).
26. Mørk, P. *Overflate og kolloidkjemi : Grunnleggende prinsipper og teorier* 8th. edition (Institutt for kjemisk prosessteknologi).

27. Wong, S. F., Lim, J. S. & Dol, S. S. Crude oil emulsion: A review on formation, classification and stability of water-in-oil emulsions. *Journal of Petroleum Science and Engineering* **135,** 498–504 (Nov. 2015).

28. Selvamani, V. in *Characterization and Biology of Nanomaterials for Drug Delivery* (eds Mohapatra, S. S., Ranjan, S., Dasgupta, N., Mishra, R. K. & Thomas, S.) 425–444 (Elsevier, Jan. 2019).

29. Destribats, M. *et al.* Soft microgels as Pickering emulsion stabilisers: role of particle deformability. *Soft Matter* **7.** Publisher: Royal Society of Chemistry, 7689–7698 (2011).

30. Chevalier, Y. & Bolzinger, M.-A. Emulsions stabilized with solid nanoparticles: Pickering emulsions. *Colloids and Surfaces A: Physicochemical and Engineering Aspects. Nanoparticles@interfaces* **439,** 23–34 (Dec. 2013).

31. McClements, D. J. in *Modern Biopolymer Science* (eds Kasapis, S., Norton, I. T. & Ubbink, J. B.) 129–166 (Academic Press, San Diego, Jan. 2009).

32. *Emulsions and Emulsion Stability* Second edition (ed Sjöblom, J.) (2006).

33. Ozan, S. C. & Jakobsen, H. A. On the effect of the approach velocity on the coalescence of fluid particles. *International Journal of Multiphase Flow* **119,** 223–236 (Oct. 2019).

34. Li, H., Wen, Y., Cao, A., Huang, J. & Zhou, Q. The influence of multivalent cations on the flocculation of activated sludge with different sludge retention times. *Water Research* **55,** 225–232 (May 2014).

35. Vajihinejad, V., Gumfekar, S. P., Bazoubandi, B., Najafabadi, Z. R. & Soares, J. B. P. Water Soluble Polymer Flocculants: Synthesis, Characterization, and Performance Assessment. *Macromolecular Materials and Engineering* **304,** 1800526 (2019).

36. Chang, Q. in *Colloid and Interface Chemistry for Water Quality Control* (ed Chang, Q.) 79–136 (Academic Press, Jan. 2016).

37. Instruments, M. *Zetasizer Nano User Manual* Aug. 2009.

38. Wang, N., Hsu, C., Zhu, L., Tseng, S. & Hsu, J.-P. Influence of metal oxide nanoparticles concentration on their zeta potential. *Journal of Colloid and Interface Science* **407,** 22–28 (Oct. 2013).

39. *Bubble pressure tensiometer — KRÜSS* Library Catalog: www.kruss-scientific.com. Nov. 2019. `https://www.kruss-scientific.com/services/education-theory/glossary/bubble-pressure-tensiometer/` (2020).

40. *Profile Analysis Tensiometer (PAT) — Institute of Physical Chemistry — University of Stuttgart* `https://www.ipc.uni-stuttgart.de/stubenrauch/equipment/pat/` (2020).
41. Benmekhbi, M., Simon, S. & Sjöblom, J. Dynamic and Rheological Properties of Span 80 at Liquid–Liquid Interfaces. *Journal of Dispersion Science and Technology* **35,** 765–776 (June 2014).
42. *Stability of suspensions for electronic applications. Application paper* 2009.
43. *Static Multiple Light Scattering applied to concentrated formulation studies* `https://www.formulaction.com/en/products-and-technologies/technologies/static-multiple-light-scattering-s-mls` (2020).
44. Shrimal, P., Jadeja, G. & Patel, S. A review on novel methodologies for drug nanoparticle preparation: Microfluidic approach. *Chemical Engineering Research and Design* **153,** 728–756 (Jan. 2020).
45. *Three-Dimensional Microfabrication Using Two-photon Polymerization* (Elsevier, 2016).
46. Ge, X. *et al.* Microfluidic technology for multiphase emulsions morphology adjustment and functional materials preparation. *Chinese Journal of Chemical Engineering* **24,** 677–692 (June 2016).
47. Teh, S.-Y., Lin, R., Hung, L.-H. & P. Lee, A. Droplet microfluidics. *Lab on a Chip* **8.** Publisher: Royal Society of Chemistry, 198–220 (2008).
48. Dudek, M., Muijlwijk, K., Schroën, K. & Øye, G. The effect of dissolved gas on coalescence of oil drops studied with microfluidics. *Journal of Colloid and Interface Science* **528,** 166–173 (Oct. 2018).
49. Bremond, N. & Bibette, J. Exploring emulsion science with microfluidics. *Soft Matter* **8.** Publisher: The Royal Society of Chemistry, 10549–10559 (Oct. 2012).
50. *SINTERFACE — Tensiometry, Tensiometer, Interfacial Tension, Interfacial Rheology, Contact angle, Zeta potential* `http://www.sinterface.com/pat1.html` (2020).
51. Dudek, M., Bertheussen, A., Dumaire, T. & Øye, G. Microfluidic tools for studying coalescence of crude oil droplets in produced water. *Chemical Engineering Science* **191,** 448–458 (Dec. 2018).
52. Zhang, Z. The flocculation mechanism and treatment of oily wastewater by flocculation. eng. *Water Science and Technology: A Journal of the International Association on Water Pollution Research* **76,** 2630–2637 (Nov. 2017).

53. Fernandes, R., Gonzalez, G. & Lucas, E. Assessment of polymeric flocculants in oily water systems. *Colloid and Polymer Science* **283,** 375–382 (2005).

Appendix

A Size measurements by dynamic light scattering

A.1 PDI for flocculants

Figure A.1 presents the average values of the measured PDI for solutions of F1-F6C obtained from the Zetasizer.

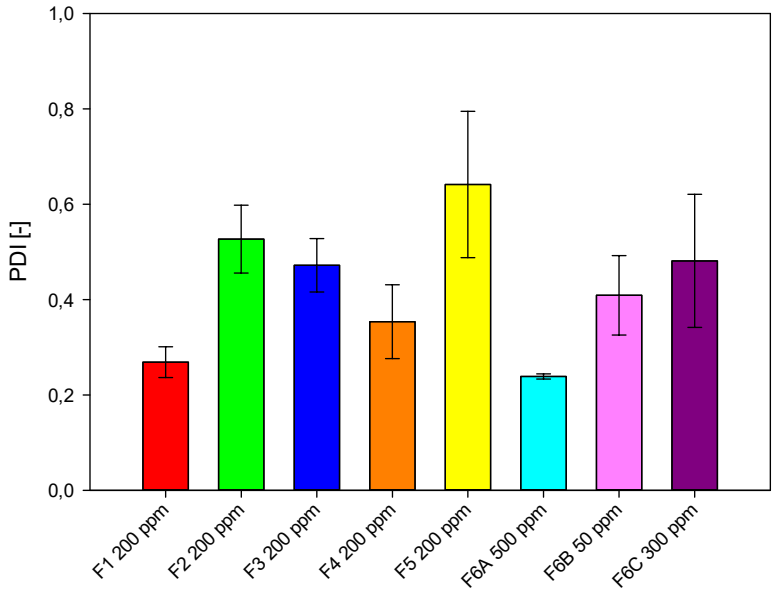

Figure A.1: PDI values for solutions of F1-F6C.

A.2 Size distribution by intensity for flocculants

Figure A.2 shows the information about number of peaks and the width of the size distributions for the measured PDI for solutions of F1-F6C, obtained from the Zetasizer.

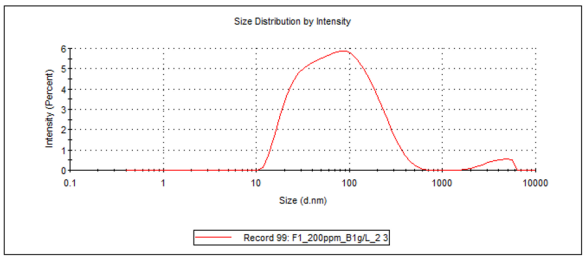

(a) F1 at 200 ppm.

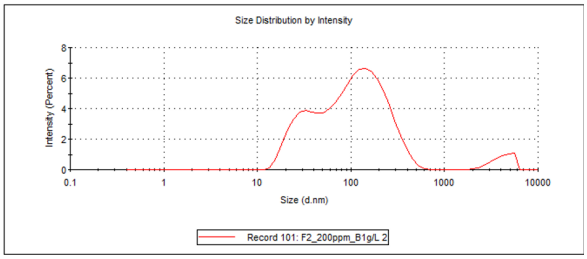

(b) F2 at 200 ppm.

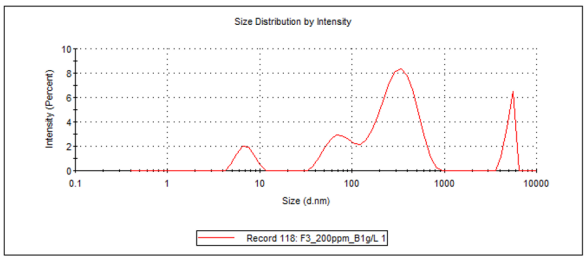

(c) F3 at 200 ppm.

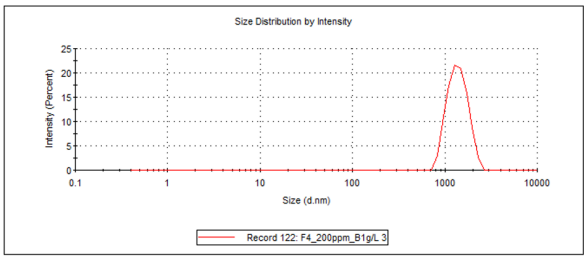

(d) F4 at 200 ppm.

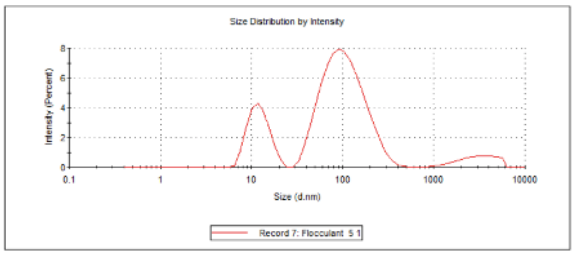

(e) F5 at 200 ppm.

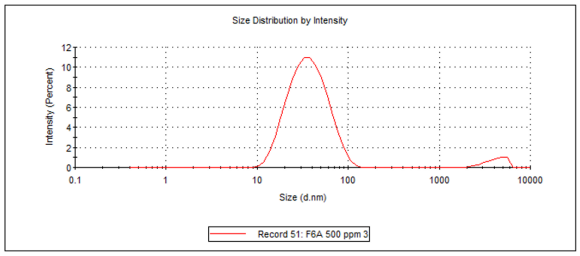

(f) F6A at 500 ppm.

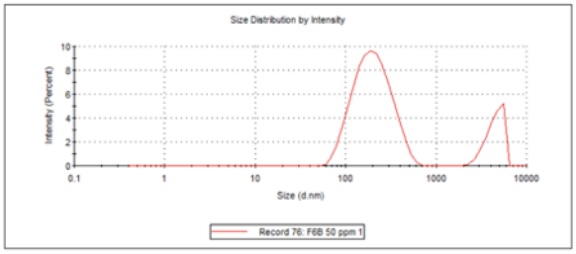

(g) F6B at 50 ppm.

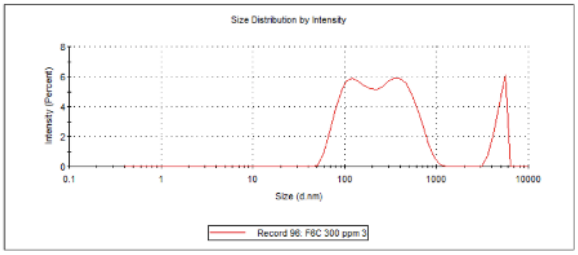

(h) F6C at 300ppm.

Figure A.2: Size distribution by intensity for solutions of F1-F6C.

B Maximum bubble pressure tensiometry

B.1 Dynamic surface tension measurements

The measured dynamic surface tension for solutions of F6A at concentrations 1000, 100, 20 and 10 ppm, measured with the BP100, is presented in Figure B.1.

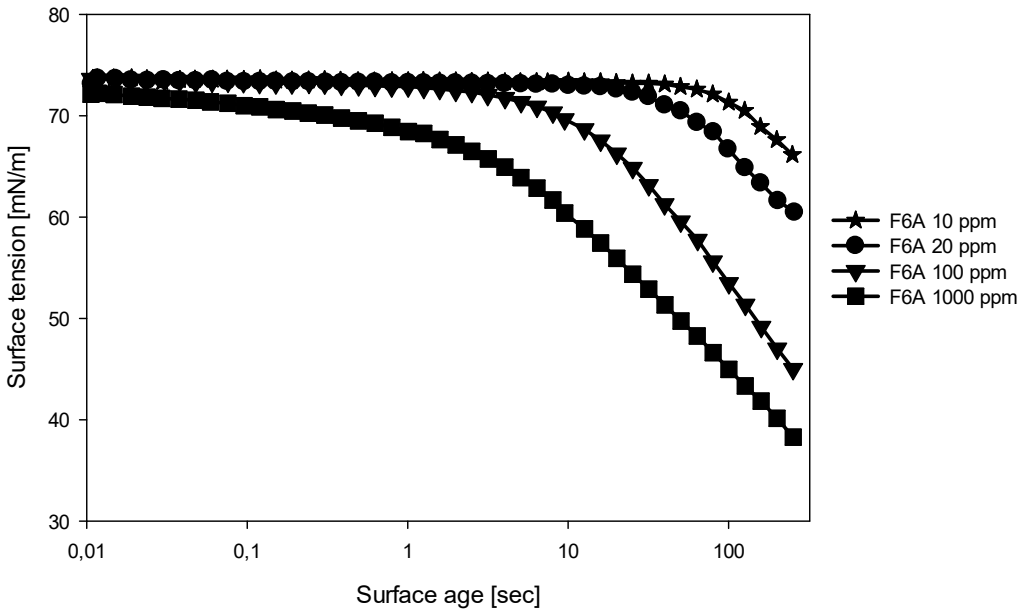

Figure B.1: Dynamic surface tension for flocculant solutions of 1000, 100, 20 and 10 ppm of F6A. The surface age on the x-axis is given in a logarithmic scale.

C Pendant drop tensiometry

C.1 Interfacial tension measurements

Figure C.1 presents the measured interfacial tension for xylene in brine with the addition of 20 ppm of F4 after 2000 seconds. The measurements were performed with the Sinterface PAT-1.

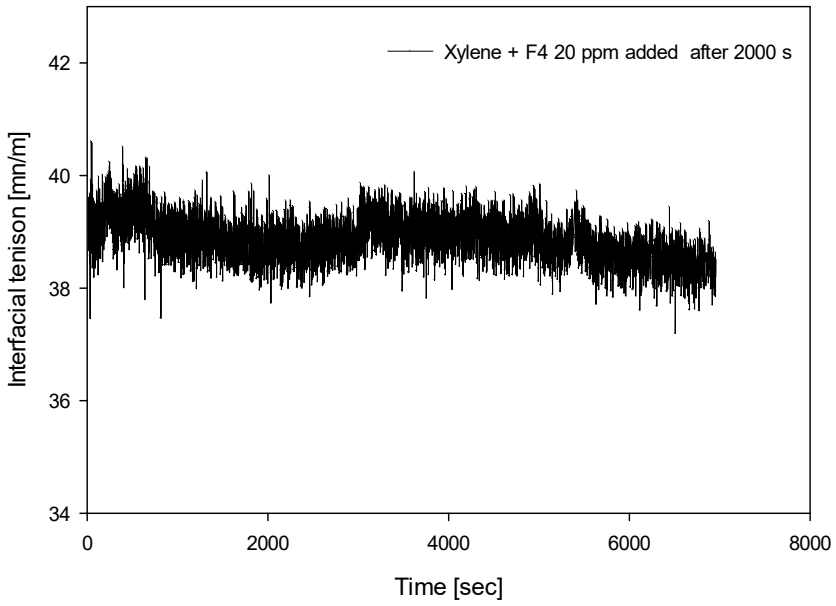

Figure C.1: Interfacial tension for xylene in brine with the addition of solution of F4 of 20 ppm after 2000 seconds.

D Microfluidics

D.1 Measurements of coalescence frequency

Figures D.1a and D.1b shows snapshots from the coalescence chamber with the addition of 5 ppm of F5 and F6A, respectively, by the use of the UMP. The snapshots shows the adsorption of oil droplets to the chip with the use of the chip design presented in Figure 4.5b in Section 4.7.2.

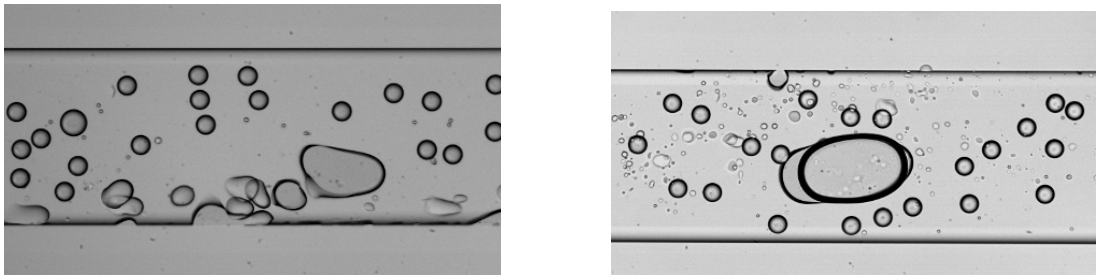

(a) F5 at 5 ppm.

(b) F6A at 5 ppm.

Figure D.1: Snapshots from the coalescence chamber.

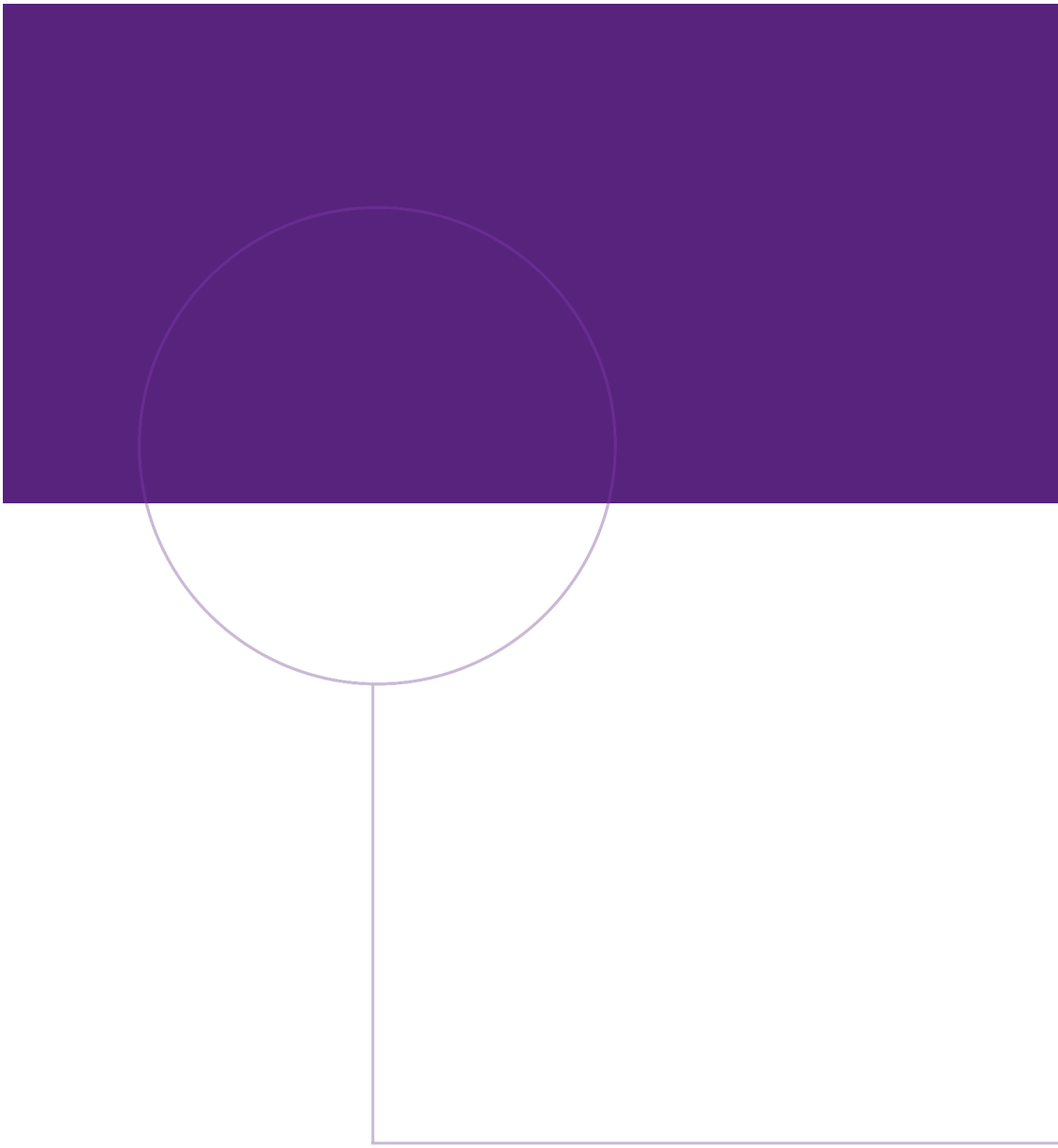

NTNU

Norwegian University of
Science and Technology